Wave-particle interaction at double resonance

A. Zaslavsky,[1] C. Krafft,[1] L. Gorbunov,[2] and A. Volokitin[3]
[1]*Laboratoire de Physique et Technologie des Plasmas, Ecole Polytechnique, 91128 Palaiseau Cedex, France*
[2]*Lebedev Physical Institute, Russian Academy of Sciences, Leninskiy Prospekt 53, 119991, Moscow, Russia*
[3]*IZMIRAN, Troitsk, Moscow Region, Russia*
(Received 29 November 2007; published 22 May 2008)

This paper is devoted to studying wave-particle interaction at "double resonance" condition, i.e., when two waves interact resonantly with the same group of charged particles. A theoretical Hamiltonian model and a symplectic numerical code are built to describe the three-dimensional interactions of wave spectra with resonant electrons in a magnetized plasma. Related simulations on the evolution of two waves of close parallel phase velocities interacting resonantly with particles' fluxes have been performed, which reveal some common features which do not depend on the kind of waves, instabilities, and particles' distributions: after the stage of linear instability, when the waves' amplitudes saturate due to particle trapping, a nonlinear process takes place which is characterized by a quasiperiodical exchange of energy between the waves, depending in particular on the value of the mismatch between the waves' resonant velocities. In order to explain such observations, a simple Hamiltonian model describing the interaction of two different waves of close resonant velocities with a periodical train of bunches of trapped particles moving synchronously has been built. It allows one to describe the nonlinear characteristics of this process as well as to estimate analytically its time scale and shows a good agreement with the numerical simulation results.

DOI: 10.1103/PhysRevE.77.056407 PACS number(s): 52.35.−g, 52.65.−y

I. INTRODUCTION

This paper is devoted to studying wave-particle interaction at "double resonance" condition, when two waves interact resonantly with the same group of charged particles in a collisionless plasma. The interest in such a problem is manifold, as discussed below.

First, the study of wave-particle interaction at double resonance can be considered as an approach to the investigation of the nonlinear stage of the so-called "sideband instability." It is well-known that an unstable monochromatic wave of frequency ω which grows in a plasma usually saturates by trapping resonant particles [1,2]. The system formed by this wave and the particles that it traps can be perturbed by the presence of other waves, with resonance velocities close to that of the main wave, that can interact with the trapped particles. In particular, a sideband instability can develop, for which the most unstable satellite waves have frequencies equal to $\omega \pm n\omega_{tr}$, where ω_{tr} is the bounce frequency of an electron oscillating in the main wave potential well and n is an integer. If among all the satellite waves one has a growth rate significantly larger than the others, the nonlinear stage of the instability can be reduced to the interaction of two waves with one group of resonant particles. Note that the sideband instability was studied analytically by considering groups of electrons with close velocities and phases interacting with two or more waves at Landau [1,3–6] and cyclotron resonances [7], as well as investigated experimentally (see, e.g., [8], and more recently [9]).

Another reason to study the problem of two or more waves interacting resonantly with the same group of particles is aimed at understanding fundamental physical processes of wave-particle interaction in plasmas which arise in the theory of nonlinear scattering of waves on particles [2,10]. In this case, one has usually to perform nonlinear perturbative calculations where third-order charge density terms present the following general structure:

$$\int d\mathbf{v} \frac{\mathbf{k}_1}{\omega_1 - \mathbf{k}_1 \cdot \mathbf{v}} \cdot \frac{\partial}{\partial \mathbf{v}} \frac{\mathbf{k}_2}{\omega_2 - \mathbf{k}_2 \cdot \mathbf{v}} \cdot \frac{\partial}{\partial \mathbf{v}} \frac{(\mathbf{k}_1 - \mathbf{k}_2)}{(\omega_1 - \omega_2) - (\mathbf{k}_1 - \mathbf{k}_2) \cdot \mathbf{v}} \cdot \frac{\partial}{\partial \mathbf{v}} f(\mathbf{v}). \quad (1)$$

Equation (1) refers to the case of two waves of frequencies ω_1 and ω_2 in an unmagnetized plasma; $\omega = \omega_1 - \omega_2$ is the frequency of one of the beating modes; $\mathbf{k}_1$, $\mathbf{k}_2$ and $\mathbf{k} = \mathbf{k}_1 - \mathbf{k}_2$ are the corresponding wave numbers; $\mathbf{v}$ is the velocity; and $f(\mathbf{v})$ usually represents the particles' velocity distribution function. It is commonly supposed that the integrations over the poles in Eq. (1) can be performed separately, taking into account the contribution of one pole only and calculating the other integrals using their principal values. It means that the number of particles which are simultaneously in resonance with each wave, that is, whose velocities $\mathbf{v}$ verify both the conditions $\omega_1 \simeq \mathbf{k}_1 \cdot \mathbf{v}$ and $\omega_2 \simeq \mathbf{k}_2 \cdot \mathbf{v}$, is smaller than the total number of particles resonantly interacting with any wave. For example, in the frame of the theory of induced scattering of waves on particles, only the pole defined by $(\omega_1 - \omega_2) - (\mathbf{k}_1 - \mathbf{k}_2) \cdot \mathbf{v} = 0$ is considered. In a plasma without ambient magnetic field and described by a Maxwellian velocity distribution, the group of particles which can be in resonant interaction simultaneously with two waves is strongly reduced. Indeed, considering the picture in the velocity space, the particles which interact resonantly with the wave $(\omega_1, \mathbf{k}_1)$ lie on a plane, whereas those interacting resonantly with the wave $(\omega_2, \mathbf{k}_2)$ lie on another one; the intersection of the two planes reduces to a straight line, where only an extremely small number of particles can interact with both waves. However, in a magnetized plasma, it is not difficult to find

two different waves with the same resonance velocities (even for the same wave branch), if one takes into account the frequency dependence on the angle between the wave vectors and the ambient magnetic field $\mathbf{B}_0$. In this case, almost all resonant particles can interact with the waves simultaneously, so that original physical features can be pointed out during the wave-particle interaction processes. Thus for the case of induced scattering on particles of two waves with the same Landau resonance velocity $v_R=\omega_1/k_{z1}\simeq\omega_2/k_{z2}$ but with different frequencies ($\omega_1\neq\omega_2$), the resonance velocity of the beating mode, $v_R'=(\omega_1-\omega_2)/(k_{z1}-k_{z2})$, coincides with v_R (k_{z1} and k_{z2} are the wave vector components directed along $\mathbf{B}_0$). Then a conventional perturbative approach to the process seems to be not adequate because the terms such as Eq. (1) contain such singularities which are not considered in the usual theory.

At last, the study of two waves interacting simultaneously with an electron beam should reveal a mechanism of nonlinear transformation of energy between the waves, through the particles. If one considers the resonant interaction of a modulated flux of energetic particles (or a periodic train of particles' bunches) with two waves of different frequencies and/or natures, there exists an interesting possibility to transfer the energy carried by one wave to the other one and, for example, to transform electrostatic energy into electromagnetic energy, or inversely. At the same time, it is possible to modify the waves' frequencies and to increase their energy densities. In our opinion, the following cases are worth studying: (i) both waves are in Landau resonance with a train of electron bunches moving with the velocity $v_z\simeq v_R=v_R'$ (v_R and v_R' are the resonance velocities of the two waves); this case is mentioned above as nonlinear induced scattering on electrons, with $v_z\simeq(\omega_1-\omega_2)/(k_{z1}-k_{z2})$; and (ii) one of the waves interacts at Landau resonance ($\omega_1=k_{z1}v_z$) with the modulated beam whereas the other one interacts with it at cyclotron resonance, $\omega_2\pm n\omega_c=k_{z2}v_z$ (ω_c is the electron cyclotron frequency); assuming that $k_{z1}=k_{z2}$ leads to the process of nonlinear (Raman) scattering at $\omega_2=\omega_1\pm n\omega_c$ on Larmor rotators.

In a magnetized plasma, the double resonance condition between two waves of resonance velocities v_{R1} and v_{R2} and a group of particles, i.e., $v_z\simeq v_{R1}\simeq v_{R2}$, can be realized in the following particular cases. A first simple example corresponds, in a strongly magnetized plasma ($\omega_p\ll\omega_c$, ω_p is the electron plasma frequency), to a quasielectrostatic lower hybrid wave and a right-polarized electromagnetic wave (whistler) with dispersion $\omega_1\simeq\omega_p k_{z1}/|\mathbf{k}_1|$ at $k_{z1}\ll|\mathbf{k}_1|$ and $\omega_2\simeq\omega_c k_{z2}^2c^2/\omega_p^2$ at $|k_{z2}|\gg|k_{2\perp}|$, respectively ($k_{2\perp}$ is the perpendicular component of the wave vector $\mathbf{k}_2$) ; the double resonance condition $v_z\simeq\omega_1/k_{z1}\simeq\omega_2/k_{z2}$ can be fulfilled for $k_{z1}\simeq k_{z2}$ if the lower hybrid wave satisfies $k_{z1}|\mathbf{k}_1|c^2\simeq\omega_p^3/\omega_c$ and $k_{z1}/|\mathbf{k}_1|\ll\omega_p/\omega_c$, which follows from $c^2|\mathbf{k}_1|^2\gg\omega_p^2$. Moreover, the parameters required to achieve the double resonance condition can be obtained more accurately by solving numerically both the resonance interaction conditions and the wave dispersion equations. Figure 1 shows the linear dispersion curves calculated for several types of waves propagating in a cold magnetized plasma, for fixed ω_c/ω_p and $k_\perp/k_z$ ($k_\perp$ is the perpendicular component of the wave vector). The two oblique lines labeled "L" and "AC" represent the Landau and the anomalous cyclotron resonance conditions, $k_z=\omega/v_z$ and $k_z=(\omega+\omega_c)/v_z$, respectively. The existence, for the same value of k_z, of crossing points between these lines and the dispersion curves of the lower hybrid and the slow extraordinary wave branches (labeled "LH" and "SX") illustrates the possibility of finding two waves interacting simultaneously with the same group of resonant particles.

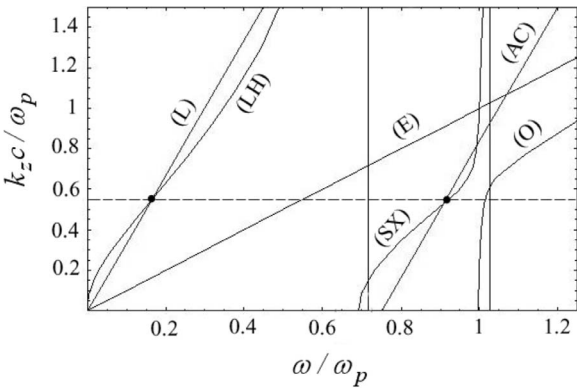

FIG. 1. Dispersion relations in a cold magnetized plasma: ck_z/ω_p as a function of ω/ω_p. The labels (LH), (SX), (O), and (E) indicate the lower hybrid, the slow extraordinary, the ordinary, and the electromagnetic light ($\omega=ck_z$) modes dispersion curves, whereas (L) and (AC) represent the Landau and the anomalous cyclotron resonance conditions, respectively; the vertical lines indicate the lower and upper hybrid frequencies. The existence of crossing points (black dots) between the horizontal line (ck_z/ω_p =const) and the curves illustrates the possibility to find a so-called "double resonance condition" for two different waves. The fixed parameters are $k_\perp/k_z=0.224$ and $\omega_c/\omega_p=0.75$.

In this paper, the double resonance problem is solved analytically using a simple one-dimensional (1D) Hamiltonian model describing the resonant interaction of two waves with the particles they trap, supposing that the particles move all quasisynchronously in the potential wells of the waves. This model allows one to describe the nonlinear characteristics of the process at work as well as to estimate analytically its time scale. Moreover, these results are shown to fit qualitatively those provided by three-dimensional (3D) numerical simulations performed by means of a symplectic code based on a Hamiltonian model describing the 3D interactions of wave spectra with resonant electrons in a magnetized plasma. The paper presents several relevant examples of physical situations where the double resonance phenomenon occurs; for example, when electrostatic waves interact (i) at Landau resonances with an electron beam (bump-on-tail instability) and (ii) at normal (anomalous) cyclotron resonances with energetic electron fluxes through ring (fan) instability. In all cases the simulations reveal that the time evolution of the amplitudes of the two waves with close resonant velocities exhibits some common features consisting of a slow and quasiperiodical exchange of energy between the waves.

The paper is organized as follows. After a short presentation of the theoretical 3D Hamiltonian model used to describe resonant wave-particle interaction in a magnetized plasma (Sec. II), we focus, in Sec. III, on the situation in

which two waves are interacting simultaneously with the same population of resonant particles. If the waves have the same (or very close) resonant velocities, we show analytically the occurrence of a nonlinear process characterized by quasiperiodical energy exchanges between the waves; these results are obtained using a Hamiltonian description where the electron population consists of bunches of trapped particles moving quasisynchronously in the waves' potential wells. Section IV presents 3D numerical simulations of wave-particle interactions under various double resonance conditions, showing that the energy exchanges predicted in Sec. III are observed. Finally, Sec. V is devoted to discuss our results and to state our conclusions; in particular, the dependence of the time scale of the nonlinear wave oscillations as a function of the electron flux intensity is considered.

II. THEORETICAL MODEL

The numerical simulation results and the analytical developments discussed in the next sections are based on a theoretical model [11,12] which describes in 3D geometry the evolution of waves resonantly interacting with particles in a magnetized plasma (nonlinear wave-wave interactions are neglected compared to wave-particle ones). Such models, the main assumptions and properties of which will be exposed in this section, have been first used in the field of plasma physics for studying the nonlinear evolution of the 1D beam-plasma instability [13,15]. They turned out to be of Hamiltonian nature [16], which enables one to study the self-consistent wave-particle interaction as a classical multidimensional mechanical system, e.g., with the help of perturbation and averaging techniques developed in the frame of Hamiltonian mechanics. Such methods were shown to be fruitful, allowing one to recover in a simple and natural way several classical plasma physics results, as the Landau growth/damping rate, for example, but also to provide interesting physical results that cannot be recovered using the usual Vlasov-Poisson approach [17,18]. A complete textbook dealing with such a Hamiltonian approach has been recently published [19], in which the interested reader can find more details. The theoretical model exposed hereafter is an extension of the 1D Hamiltonian model to 3D geometry with a magnetic field, the derivation and applications of which can be found in [11,12,17,20]. Let us now present the main features of this model.

We suppose that the plasma electrons can be divided in two groups: a bulk component (i.e., particles moving adiabatically in the field of the waves) with the density n_0, and a flux of energetic resonant particles with a much smaller average density $n_{res} \ll n_0$. The bulk component, which determines the waves' dispersion, is described in the linear approximation using hydrodynamic equations. However, the resonant particles have to be considered owing to a kinetic approach which takes into account their full nonlinear dynamics in the waves' fields.

For electrostatic oscillations in a homogeneous magnetized plasma, the electric field $\mathbf{E}$ is derived from the scalar potential $\varphi = \mathrm{Re}\ \Sigma_{\mathbf{k}} \varphi_{\mathbf{k}}(t) \exp[i(\mathbf{k}\cdot\mathbf{r} - \omega_{\mathbf{k}} t)]$, which consists in the sum of plane waves with slowly varying amplitudes $\varphi_{\mathbf{k}}(t)$, so that the average electric field energy density for the wave $(\mathbf{k}, \omega_{\mathbf{k}})$ is given by $\langle E_{\mathbf{k}}^2/8\pi \rangle = |\mathbf{k}\varphi_{\mathbf{k}}|^2/16\pi$; $\omega_{\mathbf{k}}$ is the frequency of the wave with Fourier component $E_{\mathbf{k}}$ and wave vector $\mathbf{k}$. Using a time averaging procedure to remove the fast oscillating terms from the Poisson equation [11], we obtain

$$\mathbf{k}^2 \varepsilon_{\mathbf{k}} \varphi_{\mathbf{k}} \simeq \mathbf{k}^2 \frac{\partial \varepsilon_{\mathbf{k}}}{\partial \omega_{\mathbf{k}}} (\omega - \omega_{\mathbf{k}}) \varphi_{\mathbf{k}} \simeq \mathbf{k}^2 \frac{\partial \varepsilon_{\mathbf{k}}}{\partial \omega_{\mathbf{k}}} i \frac{d}{dt} \varphi_{\mathbf{k}} \simeq -\frac{4\pi e}{V} \int_V e^{i(\omega_{\mathbf{k}} t - \mathbf{k}\cdot\mathbf{r})} \delta n_{res}(\mathbf{r}, t) d\mathbf{r}, \tag{2}$$

where $\delta n_{res}(\mathbf{r}, t)$ is the density of the resonant electrons (ions are considered as motionless); $-e < 0$ is the electron charge; $\varepsilon_{\mathbf{k}}$ is the dielectric permittivity for electrostatic waves in a cold magnetized plasma; $V = L_z L_\perp^2$ is the volume of the system which consists of a periodic box of sizes $L_z = 2\pi/k_{z\,\min}$ and $L_\perp = 2\pi/k_{\perp\,\min}$ along and across the ambient magnetic field $\mathbf{B}_0 = B_0 \mathbf{z}$, respectively ($\mathbf{z}$ is the unit vector along $\mathbf{B}_0$); k_z and $k_\perp$ are the parallel and perpendicular wave vectors, and $k_{z\,\min}$ and $k_{\perp\,\min}$ are their minimum values. Then the slow evolution of the wave amplitude $\varphi_{\mathbf{k}}(t)$ due to resonant interaction with particles is described by

$$i \frac{d}{dt} \frac{e\varphi_{\mathbf{k}}}{m_e v_*^2} \simeq -\frac{\omega_p^2}{|\mathbf{k}|^2 v_*^2} \left(\frac{\partial \varepsilon_{\mathbf{k}}}{\partial \omega_{\mathbf{k}}} \right)^{-1} \frac{2 n_{res}}{n_0} \frac{1}{N} \sum_{p=1}^{N} e^{i(\omega_{\mathbf{k}} t - \mathbf{k}\cdot\mathbf{r}_p)}, \tag{3}$$

where m_e is the electron mass; v_* is a fixed velocity used for the normalization (see below); and $\mathbf{r}_p$ is the position of the particle p. We substituted, in the Fourier transform of δn_{res}, the integral over the phase space volume by the sum on the N resonant particles located in the volume V ($N = n_{res} L_z L_\perp^2$), according to

$$\int_V e^{i(\omega_{\mathbf{k}} t - \mathbf{k}\cdot\mathbf{r})} \delta n_{res}(\mathbf{r}, t) \frac{d\mathbf{r}}{V} = \int_V \frac{d^2 r dz}{L_z L_\perp^2} \int d\mathbf{v} f_{res}(\mathbf{v}, \mathbf{r}, t) e^{i(\omega_{\mathbf{k}} t - \mathbf{k}\cdot\mathbf{r})} \to \frac{1}{N} \sum_{p=1}^{N} e^{i(\omega_{\mathbf{k}} t - \mathbf{k}\cdot\mathbf{r}_p)}. \tag{4}$$

The distribution function f_{res} of the resonant particles is normalized so that the average density is $n_{res} = \int f_{res}(\mathbf{v}, \mathbf{r}, t) d\mathbf{v} d\mathbf{r}$. The motion of an electron p is described by the Newton-Lorentz equation

$$\frac{d\mathbf{v}_p}{dt} + (\mathbf{v}_p \times \mathbf{z}) \omega_c = \frac{e}{m_e} \nabla \varphi = \frac{e}{m_e} \mathrm{Re} \sum_{\mathbf{k}} i\mathbf{k} \varphi_{\mathbf{k}}(t) e^{i(\mathbf{k}\cdot\mathbf{r}_p - \omega_{\mathbf{k}} t)},$$

$$\frac{d\mathbf{r}_p}{dt} = \mathbf{v}_p, \tag{5}$$

where $\mathbf{v}_p(\mathbf{v}_{\perp p}, v_{zp})$ is the velocity of the particle p. Equations (3) and (5) lead to the conservation of the total energy H and parallel momentum P_z of the system in the volume V:

$$\frac{d}{dt}H = \frac{d}{dt}V\left\{\frac{n_{res}}{N}\sum_p\left(\frac{m_e\mathbf{v}_p^2}{2} - e\ \mathrm{Re}\sum_{\mathbf{k}}\varphi_{\mathbf{k}}e^{i(\mathbf{k}\cdot\mathbf{r}_p-\omega_{\mathbf{k}}t)}\right) + \sum_{\mathbf{k}}W_{\mathbf{k}}\right\} = 0, \tag{6}$$

$$\frac{dP_z}{dt} = \frac{d}{dt}\left\{V\left(\sum_{\mathbf{k}}\frac{k_z}{\omega_{\mathbf{k}}}W_{\mathbf{k}} + \frac{n_{res}}{N}\sum_p m_e v_{zp}\right)\right\} = 0, \tag{7}$$

where $W_{\mathbf{k}}=\omega_{\mathbf{k}}(\partial\varepsilon_{\mathbf{k}}/\partial\omega_{\mathbf{k}})(\mathbf{k}^2|\varphi_{\mathbf{k}}|^2/16\pi)$ is the energy density of the wave $(\mathbf{k},\omega_{\mathbf{k}})$ and $m_e\mathbf{v}_p^2/2-e\ \mathrm{Re}\ \Sigma_{\mathbf{k}}\varphi_{\mathbf{k}}\exp[i(\mathbf{k}\cdot\mathbf{r}_p-\omega_{\mathbf{k}}t)]$ is the total energy of the particle p in the wave field. The dynamical system formed by Eqs. (3) and (5) can also be described using the Hamiltonian formalism developed in Appendix B (see also Refs. [12,20]), which allows one to build a symplectic numerical code for the efficient and accurate calculation of the wave-particle evolution. It allowed the authors to perform convergent calculations that ensure the conservation of the dynamical invariants of the system with a precision better than 10^{-3} whereas using time steps of the order of $\omega_c\Delta\tau=0.1-0.2$. The symplectic algorithm and mover are presented in Ref. [17].

III. ANALYTICAL INVESTIGATION OF THE DOUBLE RESONANCE PROBLEM

The purpose of this paper, as emphasized in the Introduction, is to study the situation in which two waves are interacting simultaneously with the same population of resonant particles in a magnetized plasma. First note that the wave-particle interactions at Landau resonances can be considered as 1D processes occurring along the direction of the ambient magnetic field [17], contrary to interactions at cyclotron resonances for which the perpendicular particles' motion is essential. Thus for reason of simplicity, we shall focus in this section on 1D interactions, even if the full 3D Hamiltonian presented in Appendix B allows one to treat the problem of cyclotron resonances. Moreover, the study of the physical processes at work in the 1D configuration should shed some light on the nature of the wave energy exchange mechanisms in the more complicated case of 3D geometry. Indeed, in the next section dealing with numerical simulations based on a 3D Hamiltonian model, one can observe the qualitative similarity between the process in 1D and 3D geometries.

A classical situation in which two waves are interacting with the same group of resonant particles in a plasma is the well-known sideband instability. In this case, the steady state system formed by a main wave and the particles that it traps [known as a Bernstein-Greene-Kruskal (BGK) wave [21]] is perturbed by a second wave of significantly smaller amplitude. Analytical calculations can be performed in the linear approximation [3–5], showing that the second wave (also called sideband wave) can be driven unstable and determining analytically its frequency and its maximum growth rate. In Appendix A we recover this classical result using the theoretical model presented above, under the assumption that all the particles trapped in a potential well are moving synchronously like a single macroparticle.

This assumption and the Hamiltonian nature of our model allow us to go one step further and to consider the full nonlinear interaction of two waves having nonvanishing amplitudes with a train of particle bunches. The results presented below show that there exists a stable regime for this system, in which both waves periodically exchange energy. On the basis of numerical simulations, we show in the next section that these energy exchanges can be observed in more realistic situations.

A. Two waves interacting with a train of particle bunches

Let us consider the nonlinear evolution of two waves interacting resonantly with a periodic train of electron bunches, without supposing that the waves' amplitudes are small. In order to derive analytical results, we simplify the problem by assuming that the motion of the particles in all the bunches is synchronized, which means that all the particles keep the same phases relative to the waves: the resonant particles are moving as one single macroparticle, so-called "bunch," and are described by the same dynamical variables. This is the strongest assumption done in the below developed model, and it is supported by the simulations results presented in the next section; it can be true if the parallel wavelengths of the waves are the same or if the ratio between them is an integer.

It is suitable to describe the 3D electron motion in the ambient magnetic and waves' fields with the help of the following pairs of conjugated canonical variables (see Appendixes A and B for details): the bunch's longitudinal momentum P_b and position Z_b in the laboratory frame, its angle of Larmor rotation θ_b, and its magnetic momentum J_b, as well as its guiding center in the perpendicular plane, $\mathbf{R}_{\perp b}(X_b, Y_b/m_e\omega_c)$; the dynamics of each wave α is described using the canonical action-angle variables (I_α,ϕ_α).

If one assumes that the two perpendicular wave vectors are colinear, $\mathbf{k}_{\perp 1}\times\mathbf{k}_{\perp 2}=0$, the description of the perpendicular motion of the bunch can be strongly simplified. Indeed, one observes in this case that $\mathbf{k}_\alpha\cdot\mathbf{R}_{\perp b}=\mathrm{const}$ $(\alpha=1,2)$, so that the degree of freedom associated with the perpendicular drift can be avoided. Moreover, the angles θ_α $(k_{x\alpha}=k_{\perp\alpha}\sin\theta_\alpha, k_{y\alpha}=k_{\perp\alpha}\cos\theta_\alpha)$ can also be included as initial conditions in the waves' phases. Thus after some canonical transformations (see Appendix B), the Hamiltonian $\mathcal{H}_{b,n}$ [see Eq. (B14) in Appendix B] describing a system of two waves interacting at a selected resonance n with a bunch of electrons is

$$\mathcal{H}_{b,n} = \frac{\left(\mathcal{P}-\sum_\alpha k_{z\alpha}I_\alpha\right)^2}{2M_b} + \omega_c\mathcal{J} + \sum_{\alpha=1,2}(\omega_\alpha - n\omega_c)I_\alpha - q_b\sum_{\alpha=1,2}(2\eta_\alpha I_\alpha)^{1/2}J_n(k_{\perp\alpha}\rho_b)\cos\phi_\alpha, \tag{8}$$

with

$$\phi_\alpha = \omega_\alpha t - \arg(\varphi_\alpha) - k_{z\alpha}Z_b - \mathbf{k}_\alpha\cdot\mathbf{R}_{\perp b} - n(\theta_b+\theta_\alpha), \tag{9}$$

where $M_b=N_bm_e$ and $-q_b=-N_be$ are the mass and the charge of the bunch which contains N_b particles; $\mathcal{P}$ is a constant of the motion which represents the parallel momentum of the

system [see also Eq. (B7) in Appendix B]; J_n is the Bessel function of order n; η_α is a parameter [see Eq. (B4) in Appendix B] defined as

$$\eta_\alpha = \frac{8\pi}{V\mathbf{k}_\alpha^2}\left(\frac{\partial\varepsilon(\mathbf{k}_\alpha,\omega_\alpha)}{\partial\omega_\alpha}\right)^{-1}. \tag{10}$$

The bunch's Larmor radius ρ_b in Eq. (8) can be expressed as follows:

$$\rho_b(I_\alpha) = (2J_b/M_b\omega_c)^{1/2} = \left[\frac{2}{M_b\omega_c}\left(\mathcal{J} - n\sum_\alpha I_\alpha\right)\right]^{1/2}, \tag{11}$$

where the generalized magnetic momentum $\mathcal{J}$ is a constant of the motion

$$\mathcal{J} = J_b + n\sum\nolimits_\alpha I_\alpha = \text{const}. \tag{12}$$

One can see from Eq. (8) that the parallel kinetic energy of the bunch plays the role of a wave-wave interaction energy and that the coherent motion of the bunched particles can lead to some coupling between the waves. In the case of the Landau resonance, $n=0$, one has $J_b=\mathcal{J}=$const and thus ρ_b =const. Moreover, supposing that the perpendicular wavelengths are greater than the bunch gyroradius ρ_b [$k_{\perp\alpha}\rho_b<1$, i.e., $J_0(k_{\perp\alpha}\rho_b)\simeq 1$], one can describe the system by the Hamiltonian $\mathcal{H}_{b,0}$ [see Eq. (B18) in Appendix B],

$$\mathcal{H}_{b,0} = \frac{\left(\mathcal{P} - \sum_\alpha k_{z\alpha}I_\alpha\right)^2}{2M_b} + \omega_c\mathcal{J} + \sum_{\alpha=1,2}[\omega_\alpha I_\alpha - q_b(2\eta_\alpha I_\alpha)^{1/2}\cos\phi_\alpha], \tag{13}$$

with $\phi_\alpha = \omega_\alpha t - \arg(\varphi_\alpha) - k_{z\alpha}Z_b - \mathbf{k}_\alpha\cdot\mathbf{R}_{\perp b}$. Then the Hamilton equations provide that

$$\frac{dI_\alpha}{dt} = -q_b(2\eta_\alpha I_\alpha)^{1/2}\sin\phi_\alpha, \tag{14}$$

$$\frac{d\phi_\alpha}{dt} = \omega_\alpha - \frac{k_{z\alpha}}{M_b}\left(\mathcal{P} - \sum_{\alpha=1,2} k_{z\alpha}I_\alpha\right) - q_b(\eta_\alpha/2I_\alpha)^{1/2}\cos\phi_\alpha. \tag{15}$$

B. Equilibrium and small oscillations of the system

The conditions $dI_\alpha/dt=0$ and $d\phi_\alpha/dt=0$, which determine the stationary points of Eqs. (14) and (15), impose that $\sin\phi_{1,2}=0$, i.e., $\phi_{1,2}=0$ or $\phi_{1,2}=\pi$; only the solution $\phi_{1,2}=0$ should be retained as the bunch is considered to be trapped near the bottom of the resulting potential well (stable equilibrium is considered). Then the equilibrium point (I_{1eq}, I_{2eq}) is obtained from

$$\omega_\alpha - \frac{k_{z\alpha}}{M_b}(\mathcal{P} - k_{z1}I_{1eq} - k_{z2}I_{2eq}) - q_b(\eta_\alpha/2I_{\alpha eq})^{1/2} = 0,$$

$$\alpha = 1,2. \tag{16}$$

Assuming that the potentials at equilibrium, $|\varphi_{\alpha eq}| = (2\eta_\alpha I_{\alpha eq})^{1/2}$, satisfy $|\varphi_{1eq}|\simeq|\varphi_{2eq}|\equiv|\varphi_{eq}|$ and that the frequency shift $\delta\omega_\alpha$ is small compared to ω_α,

$$\delta\omega_\alpha = -q_b(\eta_\alpha/2I_{\alpha eq})^{1/2} = -q_b\eta_\alpha|\varphi_{eq}|^{-1}, \quad |\delta\omega_\alpha| \ll \omega_\alpha, \tag{17}$$

one can write $\Delta v_\varphi = \omega_2/k_{z2} - \omega_1/k_{z1}$ in the form

$$\Delta v_\varphi = q_b(\eta_1/2k_{z1}^2 I_{1eq})^{1/2} - q_b(\eta_2/2k_{z2}^2 I_{2eq})^{1/2}, \quad |\Delta v_\varphi| \ll |v_{\varphi\alpha}|, \tag{18}$$

where $v_{\varphi\alpha}$ is the parallel phase velocity of the wave α. Then Eq. (16) imposes that both waves have very close phase velocities (i.e., whose difference Δv_φ is of the order of $\delta v_{\varphi\alpha}$). To the zeroth order in $\Delta v_\varphi/v_{\varphi\alpha}$, the equilibrium condition is given by $\delta v_{\varphi 1} = \delta v_{\varphi 2}$, which corresponds to

$$\frac{I_{1eq}}{I_{2eq}} = \frac{\eta_1}{\eta_2}\frac{k_{z2}^2}{k_{z1}^2}. \tag{19}$$

Neglecting $\delta\omega_\alpha$ compared to ω_α and defining the bunch equilibrium velocity as

$$V_{eq} = (\mathcal{P} - k_{z1}I_{1eq} - k_{z2}I_{2eq})/M_b, \tag{20}$$

one obtains from Eq. (16) that

$$\omega_\alpha - k_{z\alpha}V_{eq} \simeq 0. \tag{21}$$

Combining Eqs. (19)–(21), we get the waves' actions $I_{\alpha eq0}$ at equilibrium ($\Delta v_\varphi = 0$)

$$I_{1eq0} = \frac{\eta_1 k_{z2}}{k_{z1}}\frac{\mathcal{P} - M_b v_{\varphi 1}}{(\eta_2 k_{z1} + \eta_1 k_{z2})},$$

$$I_{2eq0} = \frac{\eta_2 k_{z1}}{k_{z2}}\frac{\mathcal{P} - M_b v_{\varphi 2}}{(\eta_2 k_{z1} + \eta_1 k_{z2})}. \tag{22}$$

Let us now determine the characteristic frequencies of the oscillations in the system and therefore examine the correction to the zero order stationary state. So let us take into account the small difference in phase velocities $|\Delta v_\varphi| \ll |v_{\varphi\alpha}|$ and assume that $I_{\alpha eq} = I_{\alpha eq0} + \delta I_{\alpha eq}$, with $|\delta I_{\alpha eq}| \ll |I_{\alpha eq0}|$. Defining $\delta\omega_{\alpha 0} = -q_b(\eta_\alpha/2I_{\alpha eq0})^{1/2}$ and $\delta v_{\varphi\alpha 0} = \delta\omega_{\alpha 0}/k_{z\alpha}$, one obtains from Eq. (18) that

$$\Delta v_\varphi \simeq \delta v_{\varphi 20}(1 - \delta I_{2eq}/2I_{2eq0}) - \delta v_{\varphi 10}(1 - \delta I_{1eq}/2I_{1eq0}), \tag{23}$$

$$\omega_\alpha + \delta\omega_{\alpha 0}(1 - \delta I_{\alpha eq}/2I_{\alpha eq0}) - k_{z\alpha}V_{eq} \simeq 0, \tag{24}$$

which leads to

$$k_{z1}\delta I_{1eq} + k_{z2}\delta I_{2eq} \simeq -M_b\delta v_{\varphi\alpha 0}(1 - \delta I_{\alpha eq}/2I_{\alpha eq0}). \tag{25}$$

Using Eqs. (23) and (25), and neglecting the third-order term proportional to $\delta v_{\varphi 20}\delta v_{\varphi 10}\delta I_{1eq}$, we find $\delta I_{\alpha eq}$,

$$\frac{\delta I_{\alpha eq}}{I_{\alpha eq0}} \simeq \frac{2k_{z\alpha'}I_{\alpha' eq0}[\Delta v_\varphi - (\delta v_{\varphi 20} - \delta v_{\varphi 10})] - M_b\delta v_{\varphi 20}\delta v_{\varphi 10}}{k_{z1}\delta v_{\varphi 20}I_{1eq0} + k_{z2}\delta v_{\varphi 10}I_{2eq0}},$$

$$\alpha, \alpha' = 1,2, \quad \alpha \neq \alpha'. \tag{26}$$

So, in the vicinity of the stationary point, the waves' amplitudes perform small oscillations described by the linearized equations ($I_\alpha = I_{\alpha eq} + \delta I_\alpha$ and $\phi_\alpha = \phi_{\alpha eq} + \delta\phi_\alpha$)

$$\frac{d}{dt}\delta I_\alpha \simeq -q_b (2\eta_\alpha I_{\alpha eq})^{1/2} \delta\phi_\alpha, \tag{27}$$

$$\frac{d}{dt}\delta\phi_\alpha \simeq \frac{k_{z\alpha}}{M_b}(k_{z1}\delta I_1 + k_{z2}\delta I_2) + q_b(\eta_\alpha/8)^{1/2} I_{\alpha eq}^{-3/2}\delta I_\alpha, \tag{28}$$

which can also be written as

$$\left[\frac{d^2}{dt^2} + \frac{q_b^2\eta_1}{2I_{1eq}} + \frac{q_b k_{z1}^2}{M_b}(2\eta_1 I_{1eq})^{1/2}\right]\delta\phi_1 \simeq -\frac{q_b k_{z1} k_{z2}}{M_b}(2\eta_2 I_{2eq})^{1/2}\delta\phi_2, \tag{29}$$

$$\left[\frac{d^2}{dt^2} + \frac{q_b^2\eta_2}{2I_{2eq}} + \frac{q_b k_{z2}^2}{M_b}(2\eta_2 I_{2eq})^{1/2}\right]\delta\phi_2 \simeq -\frac{q_b k_{z1} k_{z2}}{M_b}(2\eta_1 I_{1eq})^{1/2}\delta\phi_1. \tag{30}$$

Introducing the bounce frequencies of the bunched particles in the waves' potential as

$$\omega_{tr\alpha}^2 = \frac{e k_{z\alpha}^2}{m_e}(2\eta_\alpha I_{\alpha eq})^{1/2} = \frac{e k_{z\alpha}^2}{m_e}|\varphi_{\alpha eq}|, \tag{31}$$

and defining the frequencies

$$\omega_{x\alpha}^2 = \frac{q_b^2\eta_\alpha}{2I_{\alpha eq}} = \left[2\frac{\omega_p^2}{\omega_{tr\alpha}^2}\frac{k_{z\alpha}^2}{\mathbf{k}_\alpha^2}\left(\frac{\partial\varepsilon(\mathbf{k}_\alpha,\omega_\alpha)}{\partial\omega_\alpha}\right)^{-1}\frac{n_{res}}{n_0}\frac{N_b}{N}\right]^2, \tag{32}$$

let us search oscillatory solutions of Eqs. (29) and (30) in the form $\delta\phi_\alpha = \delta\phi_{\alpha 0} e^{i\Omega t}$. Then

$$[\omega_{x1}^2 + \omega_{tr1}^2 - \Omega^2]\delta\phi_{10} \simeq -\frac{k_{z2}}{k_{z1}}\omega_{tr1}^2\delta\phi_{20}, \tag{33}$$

$$[\omega_{x2}^2 + \omega_{tr2}^2 - \Omega^2]\delta\phi_{20} \simeq -\frac{k_{z1}}{k_{z2}}\omega_{tr2}^2\delta\phi_{10}, \tag{34}$$

providing that

$$(\omega_{x1}^2 + \omega_{tr1}^2 - \Omega^2)(\omega_{x2}^2 + \omega_{tr2}^2 - \Omega^2) \simeq \omega_{tr1}^2\omega_{tr2}^2. \tag{35}$$

The solutions $\delta\phi_\alpha$ are linear combinations of oscillations with frequencies which are roots of Eq. (35), that is, which satisfy

$$2\Omega^2 \simeq (\omega_{x1}^2 + \omega_{tr1}^2 + \omega_{x2}^2 + \omega_{tr2}^2) \pm \sqrt{(\omega_{x1}^2 + \omega_{tr1}^2 - \omega_{x2}^2 - \omega_{tr2}^2)^2 + 4\omega_{tr1}^2\omega_{tr2}^2}. \tag{36}$$

Taking into account that $\omega_{x\alpha}^2 \ll \omega_{tr\alpha}^2$, a Taylor development provides the two roots of Eq. (35),

$$\Omega_1^2 \simeq \omega_{tr1}^2 + \omega_{tr2}^2, \tag{37}$$

$$\Omega_2^2 \simeq \frac{\omega_{x1}^2\omega_{tr2}^2 + \omega_{x2}^2\omega_{tr1}^2}{\omega_{tr1}^2 + \omega_{tr2}^2} \ll \Omega_1^2. \tag{38}$$

The first regime (37) corresponds to particles oscillating at the frequency Ω_1 in the potential well formed by the two waves. The slower oscillations, which occur at a much lower frequency $\Omega_2 \propto \eta \ll \Omega_1$, reveal a more interesting phenomenon: it describes the low frequency exchanges of energy between the two waves.

C. Numerical solutions

In order to illustrate the behavior of the system over a wider range of parameters, we solved numerically Eqs. (14) and (15) for initial conditions when the bunch is trapped in the potential well of two waves with close k_z, that is, when $\mathcal{P} = N_b m_e v_\varphi + k_z(I_{10} + I_{20})$, with $I_{\alpha 0} = I_\alpha(t=0)$. All the particles are considered to be included in the bunch, i.e., $N_b/N = 1$. Close to the equilibrium, i.e., when $I_{10} \simeq I_{20}$ and $\phi_{10} \simeq \phi_{20} \simeq 0$ [$\phi_{\alpha 0} = \phi_\alpha(t=0)$], one observes the behavior predicted by the linearized equations (27) and (28): the waves' energies $I_\alpha(t)$ oscillate at the frequency Ω_2 while they are perturbed by small amplitude trapping oscillations at the frequency Ω_1.

In order to point out the influence of the bunch's phase relative to the waves, Eqs. (14) and (15) have been solved near the equilibrium point, when varying the difference of the phases of the two waves at the initial time, $\Delta\phi_0 = (\phi_{20} - \phi_{10})$ (see Fig. 2). The results show that the linear approximations (27) and (28) are valid over a large interval around the equilibrium $\Delta\phi_0 = 0$. For $|\Delta\phi_0| \simeq \pi$, the particle streams as nearly free (the parallel electric field seen by the bunch is vanishing): no periodic oscillations take place and Ω_2 cannot be defined anymore. As predicted from the solution of the linearized equations, the variation ΔI of the waves' action during the slow energy exchanges increases with $|\Delta\phi_0|$: when solving Eqs. (27) and (28) with the initial conditions $I_{10} = I_{20}$ and $\Delta\phi_0 = \phi_{20} - \phi_{10}$ one obtains that $\Delta I \simeq M_b\Omega_1^2\Delta\phi_0/\Omega_2 k_z^2$ ($k_z = k_{z1} = k_{z2}$), which fits well with the numerical results obtained within the range $-\pi/2 \lesssim \Delta\phi_0 \lesssim \pi/2$, as shown by Fig. 2. ΔI is maximum when all the electrostatic energy carried by the waves is exchanged between them through the slow oscillatory process, i.e., when $\Delta I \simeq \Delta I_{\max} = 2I_{eq}$; it follows from Eq. (22) that

$$I_{1eq} = I_{2eq} = I_{eq} \simeq (I_{10} + I_{20})/2. \tag{39}$$

The oscillations with $\Delta I \simeq \Delta I_{\max}$, which are far from the equilibrium state where $\Delta I = 0$, occur anyway with a frequency which is very close to that predicted by the linearization and take place for the initial condition $\Delta\phi_0 \simeq \pi/2$ (see Fig. 2).

Figure 3 shows the trajectories in the phase plane (ϕ_α, I_α) for $\alpha = 1$. Close to the equilibrium point (Fig. 3, left pannel), the behavior of the phase and the action is quasiregular and one can observe small amplitude fast oscillations due to the motion of the trapped particles in the bunch as well as larger amplitude oscillations corresponding to the slow energy exchanges between the waves. Near the point $|\Delta\phi_0| \simeq \pi/2$ (Fig. 3, right pannel), the trajectory (ϕ_α, I_α) is more complicated: ϕ_α increases almost linearly (with trapping oscillations of

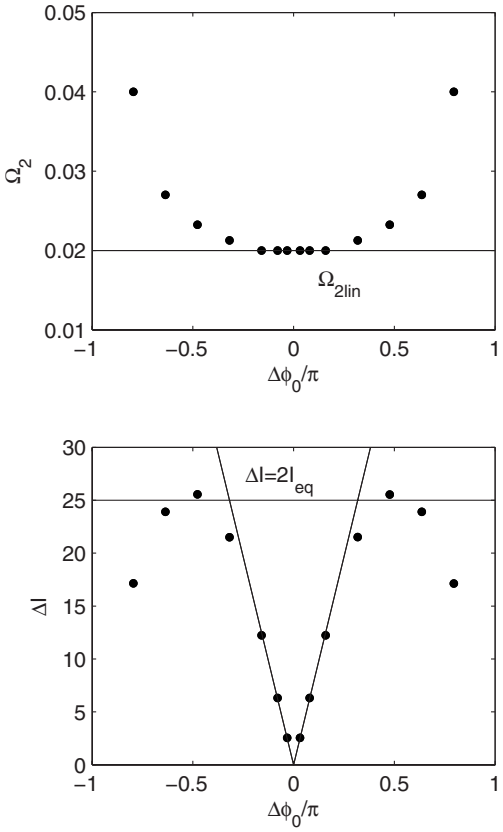

FIG. 2. Two waves of close k_z interacting with a bunch of particles at Landau resonance. Upper panel: normalized frequency Ω_2 characterizing the slow energy exchanges between the two waves [calculated by solving numerically Eqs. (14) and (15)] as a function of the difference of phases of the waves at the initial time, $\Delta\phi_0/\pi=[\arg(\varphi_{20})-\arg(\varphi_{10})]/\pi$; the horizontal line represents the normalized frequency Ω_{2lin} calculated owing to Eqs. (29) and (30). Lower panel: normalized variation ΔI of the waves' action during the slow energy exchanges, as a function of $\Delta\phi_0/\pi$; the horizontal line represents the condition $\Delta I=\Delta I_{\max}=2I_{eq}$, when all the energy is exchanged between the waves; the straight oblique lines correspond to the condition $\Delta I=M_b\Omega_1^2|\Delta\phi_0|/k_z^2\Omega_2$ (also see the text). The main normalized parameters are $M_b=1$, $q_b=1$, $k_{z1}=k_{z2}=k_z=1$, $\omega_1=\omega_2=1$, $\eta_1=\eta_2=0.01$, and $|\varphi_{10}|=|\varphi_{20}|=0.6$ (i.e., $I_{\alpha eq}\simeq 12.5$); $\arg(\varphi_{10})=0$ and $\arg(\varphi_{20})$ is varied.

very small amplitude) and consequently the action I_α behaves as a square cosinus function [as expected from Eq. (14)]. When $\phi_\alpha\to\pi/2$, i.e., $I_\alpha\to 0$ and $dI_\alpha/dt<0$, as I_α is positive, the phase jumps to the value $\phi_\alpha=-\pi/2$ due to the term proportional to $(\eta_\alpha/2I_\alpha)^{1/2}\cos\phi_\alpha\gg\Omega_2$ in Eq. (15).

IV. NUMERICAL SIMULATIONS

On the basis of the analytical investigation presented in the previous section, we now perform numerical simulations involving two electrostatic waves having the same, or very close, resonant velocities and interacting with various electron velocity distributions, for different instabilities and resonance conditions. The main attention will be paid to the physical features which are of special interest for comparison with the estimates provided by the analytical developments presented in the previous section.

In the numerical simulations, the variables are normalized as follows:

$$\mathbf{k}\to\mathbf{k}v_*/\omega_*,$$

$$\omega_{\mathbf{k}}\to\omega_{\mathbf{k}}/\omega_*,$$

$$\varphi_{\mathbf{k}}\to e\varphi_{\mathbf{k}}/m_e v_*^2, \tag{40}$$

where ω_* depends on the nature of the waves considered. Then one can present the equation of wave amplitude evolution (3) in normalized variables as

$$\frac{d}{dt}\varphi_{\mathbf{k}}=i\frac{p_*\omega_{\mathbf{k}}}{|\mathbf{k}|^2}\frac{1}{N}\sum_{p=1}^{N}e^{i(\omega_{\mathbf{k}}t-\mathbf{k}\cdot\mathbf{r}_p)}, \tag{41}$$

where p_* is a dimensionless parameter, proportional to $(n_{res}/n_0)(\partial\varepsilon_{\mathbf{k}}/\partial\omega_{\mathbf{k}})^{-1}$, which characterizes the intensity of the wave-particle interaction.

Electrostatic upper and lower hybrid waves are considered in the simulations. Their dispersion relations can be obtained from the dielectric permittivity $\varepsilon_{\mathbf{k}}$ of a magnetized plasma (here thermal effects are neglected) by solving the equation $\varepsilon_{\mathbf{k}}(\mathbf{k},\omega_{\mathbf{k}})=0$ [22], where

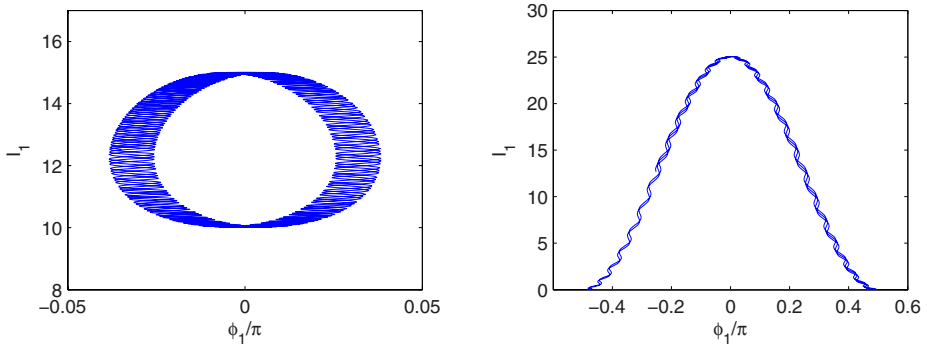

FIG. 3. (Color online) Two waves of close k_z interacting with a bunch of particles at Landau resonance. Trajectories in the phase plane (ϕ_1,I_1) showing the amplitudes of the first wave's phase and action oscillations. Left panel: the waves' initial phases are $\arg(\varphi_{10})=-\arg(\varphi_{20})=0.1$ and the system is close to its equilibrium point $|\Delta\phi_0|=0$. Right panel: the waves' initial phases are $\arg(\varphi_{10})=-\arg(\varphi_{20})=\pi/4$ and the system is near the point $|\Delta\phi_0|\simeq\pi/2$. The main parameters are the same as in Fig. 2.

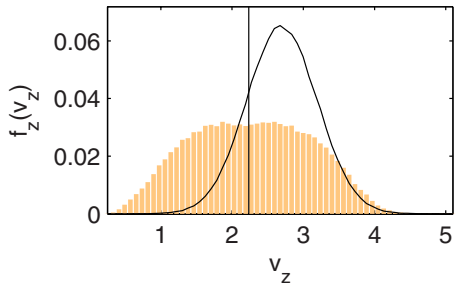

FIG. 4. (Color online) Beam instability at the Landau resonance: superposition of the initial (solid curve) and the final (gray pattern) electron parallel velocity distributions $f_z(v_z)$; v_z is the normalized parallel velocity. The vertical line indicates the normalized resonant velocities $v_{R1}=v_{R2}=2.2$ of the two lower hybrid waves. The normalized wave vectors and frequencies are $\mathbf{k}_1=(0.3,0,0.3)$, $\mathbf{k}_2=(-0.3,0,0.3)$, and $\omega_1=\omega_2=0.67$; $p_*=0.03$ [Eq. (46)]; $\omega_*=\omega_c$; $\omega_p/\omega_c=3$; and $N=200\ 000$.

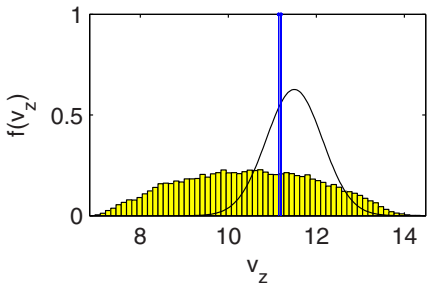

FIG. 5. (Color online) Beam instability at the Landau resonance: superposition of the initial (solid curve) and the final (gray pattern) electron parallel velocity distributions $f_z(v_z)$; v_z is the normalized parallel velocity. The vertical lines indicate the resonant velocities of the two upper hybrid waves interacting with the electrons. The normalized wave vectors and frequencies are $\mathbf{k}_1=(k_{x1},k_{y1},k_{z1})=(0.2,0.333,0.125)$, $\mathbf{k}_2=(k_{x2},k_{y2},k_{z2})=(-0.2,0.333,0.125)$; $\omega_1=\omega_2=1.4$; $p_*=0.05$ [Eq. (44)]; $\omega_*=\omega_p$; and $N=100\ 000$.

$$\varepsilon_{\mathbf{k}}=1-\frac{\omega_p^2}{\omega_{\mathbf{k}}^2}\frac{k_z^2}{\mathbf{k}^2}+\frac{\omega_p^2}{\omega_c^2-\omega_{\mathbf{k}}^2}\frac{k_\perp^2}{\mathbf{k}^2}-\frac{\omega_{pi}^2}{\omega_{\mathbf{k}}^2}. \tag{42}$$

For a weakly magnetized plasma ($\omega_p \gg \omega_c$), the upper hybrid waves propagate with the dispersion

$$\omega_{\mathbf{k}}^2 \simeq \omega_p^2\left(1+\frac{\omega_c^2}{\omega_p^2}\frac{\mathbf{k}_\perp^2}{\mathbf{k}^2}\right), \tag{43}$$

and $\partial\varepsilon_{\mathbf{k}}/\partial\omega_{\mathbf{k}} \simeq 2/\omega_{\mathbf{k}}$. In this case, $\omega_*=\omega_p$ and the corresponding parameter p_* in Eq. (41) is

$$p_*=\frac{n_{res}}{n_0} \ll 1. \tag{44}$$

Lower hybrid waves propagate in the frequency range $\omega_{lh}=\omega_{pi}\omega_c/(\omega_c^2+\omega_p^2)^{1/2} \ll \omega_{\mathbf{k}} \leq \omega_c$ (at arbitrary ω_c/ω_p) with the approximate dispersion relation

$$\frac{\omega_{\mathbf{k}}^2}{\omega_c^2} \simeq \frac{\omega_p^2}{\omega_c^2+\omega_p^2}\frac{k_z^2}{\mathbf{k}^2}, \tag{45}$$

and $\partial\varepsilon_{\mathbf{k}}/\partial\omega_{\mathbf{k}} \simeq 2(\omega_c^2+\omega_p^2)/\omega_{\mathbf{k}}\omega_c^2$, so that, choosing the normalization frequency $\omega_*=\omega_c$ in Eq. (41), we have

$$p_*=\frac{\omega_p^2}{\omega_c^2+\omega_p^2}\frac{n_{res}}{n_0} \ll 1. \tag{46}$$

As shown by the form of the dispersion relations (43) and (45), and due to the azimuthal symmetry of the magnetized plasma considered, all the waves which have the same k_z and $|\mathbf{k}_\perp|$ have also the same resonance velocity $v_R=(\omega_{\mathbf{k}}-n\omega_c)/k_z$. It is clear that small differences between the frequencies and the perpendicular wave vectors of such waves can exist without violating the equality of their resonance velocities. Various electron distributions have been chosen in order to study wave excitation by different instabilities and resonance conditions; we considered mainly the case when the initial parallel distribution $f_z(v_z)$ of the resonant particles consists in a beam. Figures 4 and 5 show the distribution $f_z(v_z)$ resulting from the particles' interaction with two waves $(\omega_1,\mathbf{k}_1)$ and $(\omega_2,\mathbf{k}_2)$; its evolution with time is typical of the so-called bump-on-tail instability of a single wave in the hydrodynamic regime (see, e.g., [1]). Thus the velocity distribution at the saturation stage appears not to depend essentially on the fact that two waves (and not only one) are interacting with the beam at the same resonant velocity.

At this step, let us remind some relevant features characterizing the spatial self-organization of the resonant particles during their interaction with a single wave. If the instability is of hydrodynamic type, most of the trapped particles form a train of bunches periodically distributed in space. All particles have close phases relative to the wave and oscillate synchronously near the bottom of its potential well. When the instability is of kinetic type, only a small part of the total amount of trapped particles forms the bunch and most of them oscillate in the well with different frequencies; after some time, phase mixing occurs and the particles stop to exchange energy with the wave on average. In this state the amplitude of the wave is roughly constant and it can be considered as a Bernstein-Green-Kruskal mode (see, e.g., [21]). For intermediate cases between the hydrodynamic and the kinetic regimes, a relatively small amount of particles move in the well with correlated phases, forming a long time living bunch, which in turn supports the wave's amplitude oscillations around a saturation level in the asymptotic interaction stage. In our paper, we consider mainly the situation when a significant part of the trapped particles form a well-structured bunch (quasihydrodynamic regime).

Figure 6 shows the variation with time of the square field amplitudes $|\mathbf{E}_{\mathbf{k}}|^2$ and of the phase mismatch $\Delta\phi_{\mathbf{k}}=\arg(\varphi_{\mathbf{k}_1})-\arg(\varphi_{\mathbf{k}_2})$ of two lower hybrid waves $(\omega_1,\mathbf{k}_1)$ and $(\omega_2,\mathbf{k}_2)$; note that $\Delta\phi_{\mathbf{k}}$ is equal, with accuracy of a constant, to the difference of the generalized phases $\phi_{1,2}$ defined by Eq. (9). The initial values of $\Delta\phi_{\mathbf{k}}$ have been chosen arbitrarily and differ for each simulation. Due to the beam instability, both waves' amplitudes grow exponentially and saturate due to trapping of electrons [14,15]. If the two waves behave independently, the time variation of $|\mathbf{E}_{\mathbf{k}}|^2$ should present, for each wave, small trapping oscillations around a roughly constant saturation level. Instead of this, as the two resonant wave velocities are equal ($\Delta v_R=v_{R1}-v_{R2}=\omega_2/k_{z2}-\omega_1/k_{z1}=0$), one observes the nontrivial interaction predicted in Sec. III be-

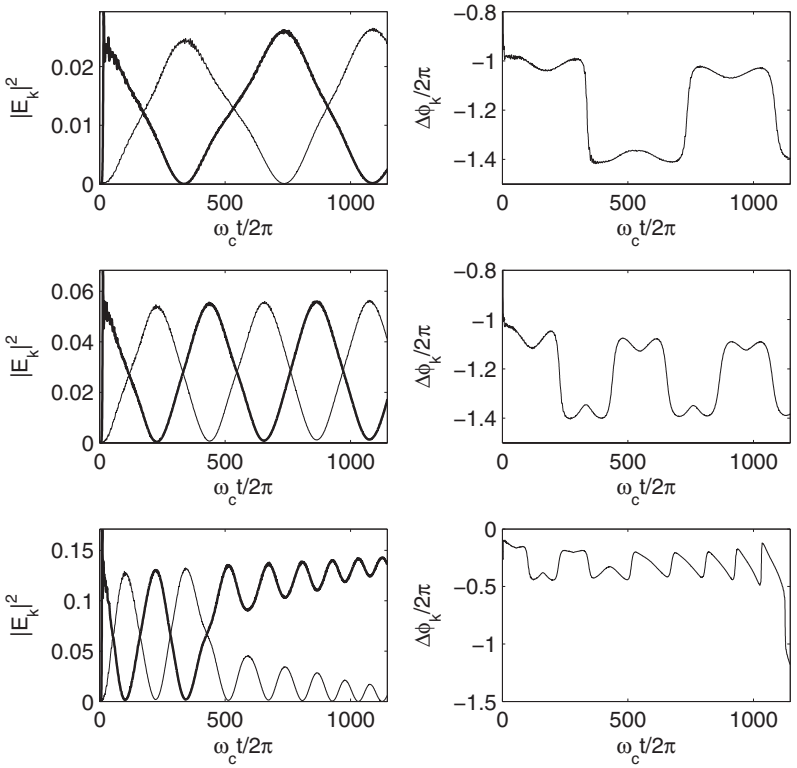

FIG. 6. Beam instability at the Landau resonance: variation as a function of the time $\omega_c t/2\pi$ of the normalized square field amplitudes $|\mathbf{E}_\mathbf{k}|^2$ (left panels) and of the relative phases $\Delta\phi_\mathbf{k}/2\pi$ (right panels) of two lower hybrid waves, for $p_*=0.02$, 0.03, and 0.05 (from the upper to the lower panels, respectively). Both waves have the same phase velocity, $\Delta v_R = v_{R1} - v_{R2} = 0$. The first wave $(\omega_1, \mathbf{k}_1)$ [the second wave $(\omega_2, \mathbf{k}_2)$] is represented as a black solid [thin] line. The electron velocity distribution and the waves are the same as in Fig. 4.

tween the waves and the resonant particles, that is, the development of quasiperiodic exchanges of energy between the two waves. The phase mismatch $\Delta\phi_\mathbf{k}$ also performs oscillations, with the same periodicity, around a constant value. The same process of energy exchanges between two waves has been evidenced for upper hybrid waves interacting with electrons at Landau resonance, as shown by Fig. 7.

This energy exchange process is sensitive to the level of nonlinearity [i.e., to the flux intensity p_* defined in Eqs. (44) and (46)] as well as to other parameters, as the direction of the wave vectors in the plane perpendicular to $\mathbf{B}_0$ or the velocity mismatch $\Delta v_R = v_{R1} - v_{R2}$. Figure 8 shows the time variation of $|\mathbf{E}_\mathbf{k}|^2$ for several values of Δv_R, revealing different oscillatory behaviors, whose periods decrease when Δv_R

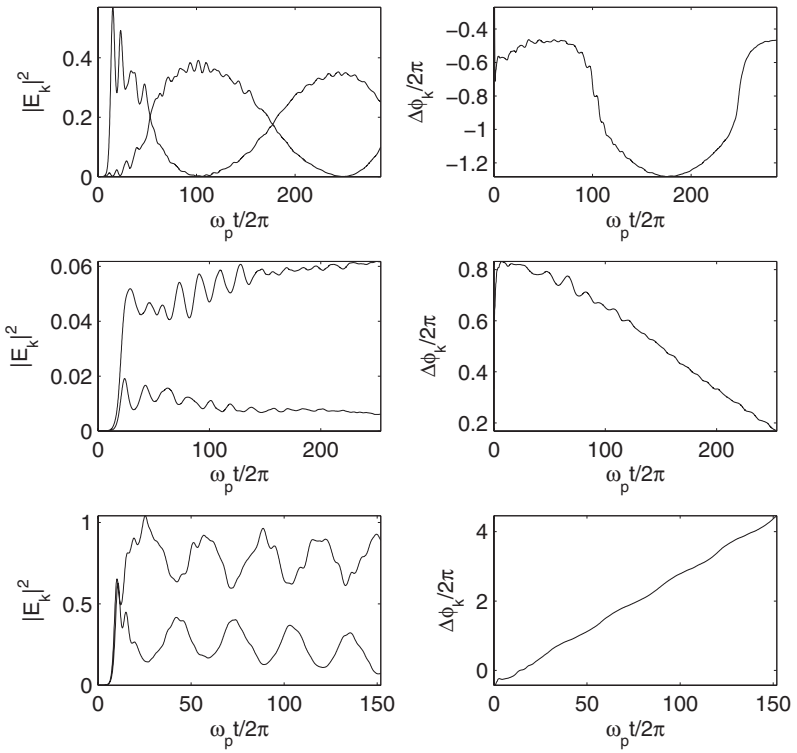

FIG. 7. Beam instability at Landau resonance: variation as a function of the time $\omega_p t/2\pi$ of the normalized square field amplitudes $|\mathbf{E}_\mathbf{k}|^2$ (left panels) and of the relative phases $\Delta\phi_\mathbf{k}/2\pi$ (right panels) of two upper hybrid waves, for three different cases: (i) upper panels: normalized frequencies and wave vectors are $\omega_1=\omega_2=1.4$, $\mathbf{k}_1=(0.2, 0.333, 0.125)$, $\mathbf{k}_2=(-0.2, 0.333, 0.125)$, and $\Delta v_R=0$, $p_*=0.05$, $N=100\ 000$; (ii) middle panels: same as (i) but $p_*=0.02$; and (iii) lower panels: the two waves present a small phase velocity mismatch $\Delta v_R \simeq 0.05$, with the normalized phase velocity $v_{R1,2}=\omega_{1,2}/k_{z1,2}\simeq 11.2$; $\omega_1=1.39$, $\omega_2=1.4$, $\mathbf{k}_1=(0.2, 0.286, 0.125)$, $\mathbf{k}_2=(0.4, 0.143, 0.125)$; $p_*=0.1$; and $N=100\ 000$. The electron velocity distribution is the same as in Fig. 6.

increases. Note that for an extremely small value of Δv_R ($\Delta v_R/v_R \simeq 0.005$), the period of the energy exchanges is divided by a factor of 2 compared to the case when $\Delta v_R=0$, and the oscillations are no more symmetric. For larger values (that is, when $\Delta v_R/v_R \simeq 0.01-0.02$), the waves' amplitudes perform oscillations of smaller amplitude and period—different from the trapping oscillations—around some average value. This feature, as well as the dependence on p_*, are coherent with the analytical results presented above, based on the hypothesis that a coherent particle bunch formed during the instability process [15] is simultaneously trapped in the potential wells of the two waves.

One should note that the oscillatory behavior which takes place during the saturation stage of the wave-particle instability does not depend on the kind of waves considered in the simulations: the same qualitative behavior is observed for the upper hybrid waves (Figs. 5 and 7) and for the lower hybrid waves (Figs. 4, 6, and 8). Moreover, even if this case has not been explicitly investigated in the previous section, simulations of lower hybrid waves destabilized at cyclotron resonances by other types of instabilities have also been performed. Relevant results are sketched in Figs. 9–12 for the fan (ring) instability at the anomalous (normal) cyclotron resonance (see [11,12,23] and [24]), showing similar behaviors of the wave-particle system: after a stage of exponential growth, the instability saturates due to trapping of resonant particles, after which very slow (compared to the bounce period ω_{tr}^{-1}) exchanges of energy occur between the two waves. Note that the simulation results agree with those provided by the numerical solution of the equations presented in the previous section, for the case when the waves exchange between each other almost all their energy.

Finally, note that in Figs. 6–8 and 10 the saturation level of one of the waves' amplitudes (just after the linear stage of the instability) is much larger than that of the other wave. This feature can be explained by the mechanism of particle trapping: when a wave gets enough energy to trap a large amount of electrons, the perturbations of their motion due to trapping cause the linear growth of the other wave to saturate (as both waves are sharing the same population of resonant particles). The random fluctuations (Schottky noise) that determine the amplitude of the waves before the instability occurred are responsible for the fact that one wave traps electrons before the other. Anyway, it occurs also that both waves saturate around the same level of energy, in particular for the fan instability case, as shown in Fig. 11.

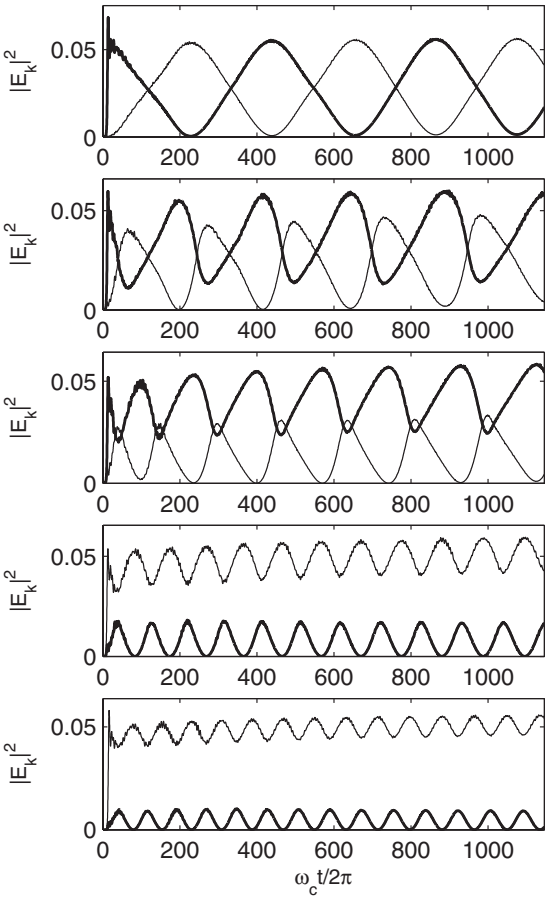

FIG. 8. Beam instability at Landau resonance: variation as a function of $\omega_c t/2\pi$ of the normalized square field amplitudes $|\mathbf{E_k}|^2$ of two lower hybrid waves, for different resonant velocity mismatches Δv_R between the waves. The parameters are the same as in Fig. 4, except of the second wave for which the perpendicular wave vector $k_{\perp 2}=|k_{x2}|$ varies as follows (from the upper to the lower panel): $k_{x2}=-0.300$, -0.303, -0.305, -0.307, and -0.310, corresponding to $\Delta v_R/v_R=0$, 0.005, 0.008, 0.011, and 0.016, respectively. The first wave $(\omega_1,\mathbf{k}_1)$ [the second wave $(\omega_2,\mathbf{k}_2)$] is represented by a solid [thin] line. The electron velocity distribution and the waves are the same as in Fig. 4.

V. DISCUSSION AND CONCLUSION

The same oscillatory behavior characterizing the variation with time of the waves' amplitudes has been shown, at least qualitatively, to result from the 3D simulations and from the numerical solution of Eqs. (14) and (15) for $|\Delta\phi_0| \simeq \pi/2$ (i.e., when the waves exchange between each other almost all their energy). Let us now compare in more details the analytical results derived in Sec. III and the numerical simulations of Sec. IV. One of the most interesting parameters is the time period $T_2=2\pi/\Omega_2$ characterizing the slow energy exchanges between the waves. In order to obtain clear power laws for T_2 as a function of the basic physical parameters, let us choose two waves which differ one from the other only by the direction of their perpendicular wave vectors $\mathbf{k}_{\perp\alpha}$ (so they have the same $k_{z\alpha}$, η_α, and $k_{\perp\alpha}$).

For lower hybrid waves, Eqs. (10), (45), and (46) lead to

$$\eta_\alpha = \frac{4\pi}{V}\frac{\omega_c^2}{\omega_c^2+\omega_p^2}\frac{\omega_\alpha}{\mathbf{k}_\alpha^2} = \frac{4\pi n_0}{N}\frac{\omega_c^2}{\omega_p^2}\frac{p_*\omega_\alpha}{\mathbf{k}_\alpha^2}, \tag{47}$$

so that the frequency Ω_2 defined in Eq. (38) can be expressed as

$$\Omega_2 = \frac{q_b\eta_\alpha}{|\varphi_{eq}|} = \frac{\omega_c^2 m_e}{e|\varphi_{eq}|}\frac{p_*\omega_\alpha}{\mathbf{k}_\alpha^2}\frac{N_b}{N}, \tag{48}$$

where we took into account that $q_b=eN_b$ and $|\varphi_{eq}| = (2\eta I_{eq})^{1/2} = [(|\varphi_{10}|^2+|\varphi_{20}|^2)/2]^{1/2}$.

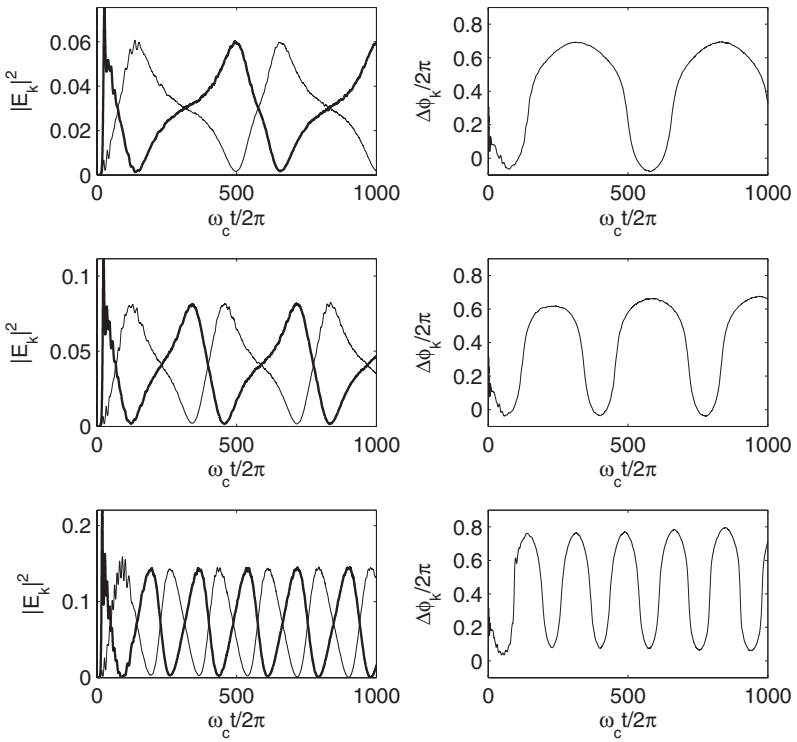

FIG. 9. Ring instability at the normal cyclotron resonance: variation as a function of $\omega_c t/2\pi$ of the normalized square field amplitudes $|\mathbf{E}_\mathbf{k}|^2$ of two lower hybrid waves (left panels) and of their relative phases $\Delta\phi_\mathbf{k}/2\pi$ (right panels), for $p_*=0.04$, 0.05, and 0.08 (from the upper to the lower panels, respectively). The first wave $(\omega_1,\mathbf{k}_1)$ [the second wave $(\omega_2,\mathbf{k}_2)$] is represented by a solid [thin] line. The normalized parameters are $\omega_1=\omega_2=0.41$, $\mathbf{k}_1=(0.3,0,-0.14)$, $\mathbf{k}_2=(-0.3,0,-0.14)$, $\omega_p/\omega_c=3$, and $N=200\ 000$.

First, in order to determine the power β of the scaling law $T_2\propto p_*^\beta$ using the 3D numerical simulations, we considered the simple case when the two waves have finite initial amplitudes (i.e., much larger than the wave thermal energy or the Schottky noise), whereas an electron beam—with a small enough density to avoid wave amplification—is launched with a velocity equal to the waves' phase velocities. In this case, the waves' amplitudes are oscillating regularly and Fig. 13 shows the variation of $\omega_c T_2/2\pi$ as a function of p_*, the initial waves' amplitudes being kept constant when varying p_*. The dots represent the results provided by the 3D numerical simulations, whereas the straight line indicates the analytical estimate derived from Eq. (48), where $N_b/N\simeq 0.08$ has been chosen so that the theoretical curve fits quantitatively the simulation data. When the formed bunch results from the instability of a beam initially homogeneous in space, not all the bunched particles are moving with a perfect synchronism, some of them are being totally phase mixed. So N_b/N should be understood as the approximate proportion of bunched particles with respect to the total number of particles. Note that in this case, the scaling $T_2\propto p_*^{-1}$ is verified, under the assumption that N_b/N does not depend on p_*.

The more complicated situation, when the energy exchanges between the waves take place during the saturation stage of the instability, has also been investigated numerically. In this case, the bunch is created by the instability mechanism and the motion of the bunched particles remains coherent during a long time (i.e., compared to the bounce period of the trapped particles in the waves' potential well). As discussed previously, the waves' action at equilibrium, I_{eq}, is approximately equal to the average value of the saturated waves' action [i.e., Eq. (39) is still valid when replacing $I_{\alpha 0}$ by $I_{\alpha s}$, where $I_{\alpha s}$ is the action of the wave α at saturation], as the bunch formed by the trapped particles obviously

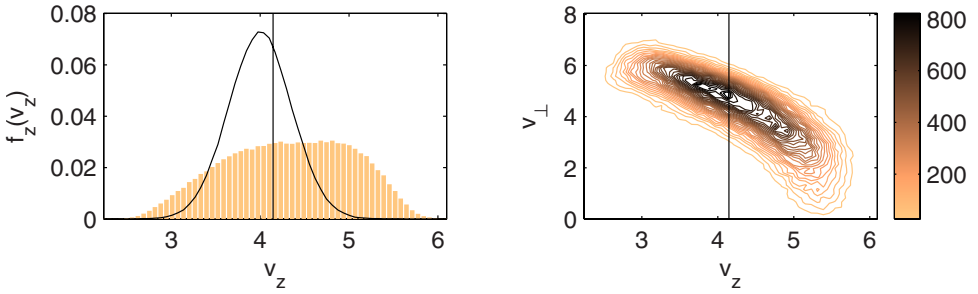

FIG. 10. (Color online) Ring instability at the normal cyclotron resonance. Left panel: superposition of the initial (solid curve) and the final (gray pattern) velocity distributions $f_z(v_z)$. The vertical line indicates the normalized resonance velocity of the two lower hybrid waves, $v_{R1}=v_{R2}=(\omega_\mathbf{k}-\omega_c)/k_z=4.1$. The initial distribution function consists of a beam drifting along the parallel and perpendicular directions with the normalized drift velocities $v_{zb}=4$ and $v_{\perp b}=5$, respectively; corresponding thermal velocities are $v_{thz}=v_{th\perp}=0.7$. Right panel: phase space $(v_z,v_\perp)$ at the final simulation time. The parameters are the same as in Fig. 9, for $p_*=0.05$.

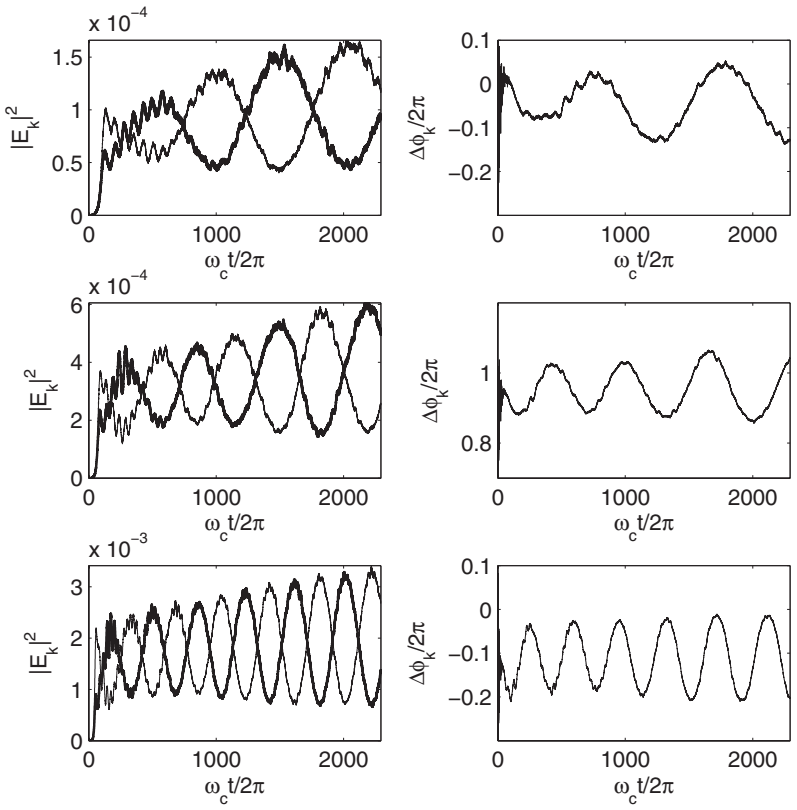

FIG. 11. Fan instability at the anomalous cyclotron resonance: variation as a function of $\omega_c t/2\pi$ of the normalized squared field amplitudes $|\mathbf{E}_\mathbf{k}|^2$ of two lower hybrid waves (left panels) and of their relative phases $\Delta\phi_\mathbf{k}/2\pi$ (right panels), for $p_*=0.02$, 0.03, and 0.05 (from the upper to the lower panel, respectively). The first wave $(\omega_1,\mathbf{k}_1)$ [the second wave $(\omega_2,\mathbf{k}_2)$] is represented by a solid [thin] line. The normalized parameters are $\mathbf{k}_1=(0.3,0,0.3)$, $\mathbf{k}_2=(-0.3,0,0.3)$, $\omega_1=\omega_2=0.67$, $\omega_p/\omega_c=3$, and $N=200\ 000$.

moves with a parallel velocity approximately equal to $v_{\varphi\alpha}=\omega_\alpha/k_{z\alpha}$, at the bottom of the potential well of the saturated waves.

Let us now determine the scaling law of T_2 using the numerical simulations of two unstable driven lower hybrid waves interacting with a train of bunches. One can expect that the equilibrium values I_{eq} of the waves' actions at saturation should be related to the flux intensity p_* [11,12]. The upper (lower) panels of Fig. 14 present the variations of T_2 $(|\varphi_\mathbf{k}|^2_{eq})$ as a function of p_*, for beam, fan, and ring instabilities, showing that the results are coherent with the estimates of Ref. [11], obtained using the conservation of the parallel momentum of the wave-particle system (B7) and the assumption that the linear growth rate of the instability must vanish at wave saturation. For the fan instability, the simulation results are in good agreement with the analytical predictions, that is, $|\varphi_\mathbf{k}|^2_{eq}=(|\varphi_{\mathbf{k}_1}|^2_s+|\varphi_{\mathbf{k}_2}|^2_s)/2\propto p_*^3$ ($|\varphi_\mathbf{k}|_s$ is the potential at saturation) and $T_2\propto p_*^{-1}$. For the beam and the ring instabilities, two regimes have to be distinguished. Indeed, for $p_*\lesssim 0.01$, only a small part of the beam particles strongly interact with the waves (kinetic limit of the wave-particle interaction); for larger values of p_* ($p_*\gtrsim 0.03$), nearly all the particles are trapped coherently by the waves (hydrodynamic limit when all the particles are moving like a single macroparticle in the waves' potential well). For the beam instability, no simple power law can be determined: for large p, the numerical simulations provide that $|\varphi_\mathbf{k}|^2_{eq}\propto p_*^{1.7}$, which is not far from what is obtained analytically by considering a purely hydrodynamic instability (i.e., $|\varphi_\mathbf{k}|^2_{eq}\propto p_*^{4/3}$ [11]); note that our values of p_* are not small enough to allow us to investigate the range of purely kinetic regime where $|\varphi_\mathbf{k}|^2_{eq}\propto p_*^4$ [11]. For the ring instability, the power laws

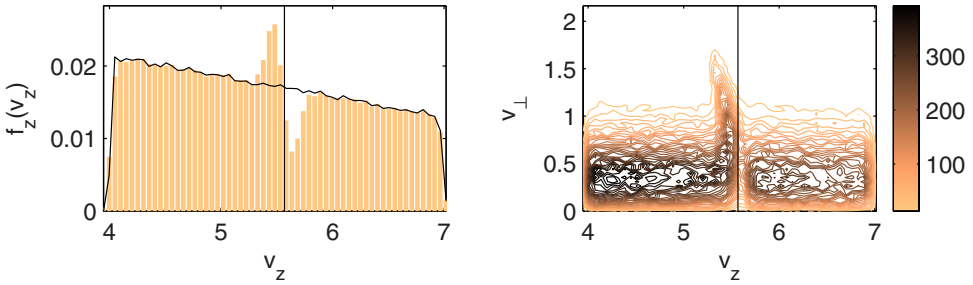

FIG. 12. (Color online) Fan instability at the anomalous cyclotron resonance. Left panel: superposition of the initial (solid curve) and the final (gray pattern) velocity distributions $f_z(v_z)$. The vertical line indicates the normalized resonance velocity of the two lower hybrid waves, $v_{R1}=v_{R2}=(\omega_\mathbf{k}+\omega_c)/k_z=5.6$. The initial distribution function consists in a nearly flat suprathermal tail extending from $v_z=4$ to 7 in the parallel direction and in a Maxwellian of thermal velocity $v_{th\perp}=0.7$ in the perpendicular direction. Right panel: phase space $(v_z,v_\perp)$ at the final simulation time. The parameters are the same as in Fig. 11, for $p_*=0.03$.

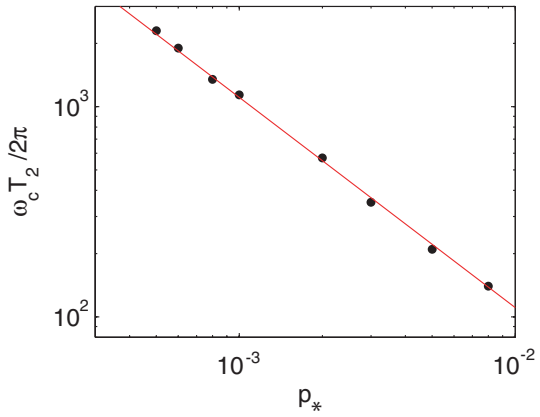

FIG. 13. (Color online) Interaction between two lower hybrid waves and an electron beam: variation of the normalized period $\omega_c T_2/2\pi$ of the energy exchanges between the waves as a function of the flux intensity p_* [Eq. (46)]. The dots correspond to the results provided by 3D numerical simulations and the straight line to the theoretical estimate of T_2 [Eq. (48)] (N_b/N being fixed to 0.08, as explained in the text). The initial waves' amplitudes are $|\varphi_{10}|=1.0$ and $|\varphi_{20}|=0.1$. The main normalized parameters are $\mathbf{k}_1=(0.2,0,0.1)$, $\mathbf{k}_2=(-0.2,0,0.1)$, and $\omega_1=\omega_2=0.42$.

$|\varphi_{\mathbf{k}}|^2_{eq} \propto p_*^{2.5}$ and $|\varphi_{\mathbf{k}}|^2_{eq} \propto p_*^{1.2}$ obtained numerically for the kinetic and hydrodynamic regimes are not very far from the corresponding theoretical estimates, that is, $|\varphi_{\mathbf{k}}|^2_{eq} \propto p_*^3$ and $|\varphi_{\mathbf{k}}|^2_{eq} \propto p_*^2$, respectively [11].

Moreover, one can write using Eq. (48) that

$$\Omega_2(p_*) \propto \frac{p_*}{|\varphi_{eq}(p_*)|}\frac{N_b(p_*)}{N}, \tag{49}$$

and, owing to the power laws obtained above, one can determine the scaling of T_2. Then, for the beam instability, the period $T_{2b} \equiv T_2$ scales as

$$T_{2b,h} \propto p_*^{-0.15}\frac{N}{N_b(p_*)},$$

$$T_{2b,k} \propto p_*^{0.25}\frac{N}{N_b(p_*)}, \tag{50}$$

where the subscripts h and k indicate the hydrodynamic and the kinetic regimes, respectively. Supposing that Eq. (48) is also valid for instabilities taking place at the cyclotron resonances—we are aware that this assumption is not obvious at all—one gets for the fan instability ($T_{2f} \equiv T_2$)

$$T_{2f,k} \propto p_*^{0.5}\frac{N}{N_b(p_*)}, \tag{51}$$

and for the ring instability ($T_{2r} \equiv T_2$)

$$T_{2r,h} \propto p_*^{0.4}\frac{N}{N_b(p_*)},$$

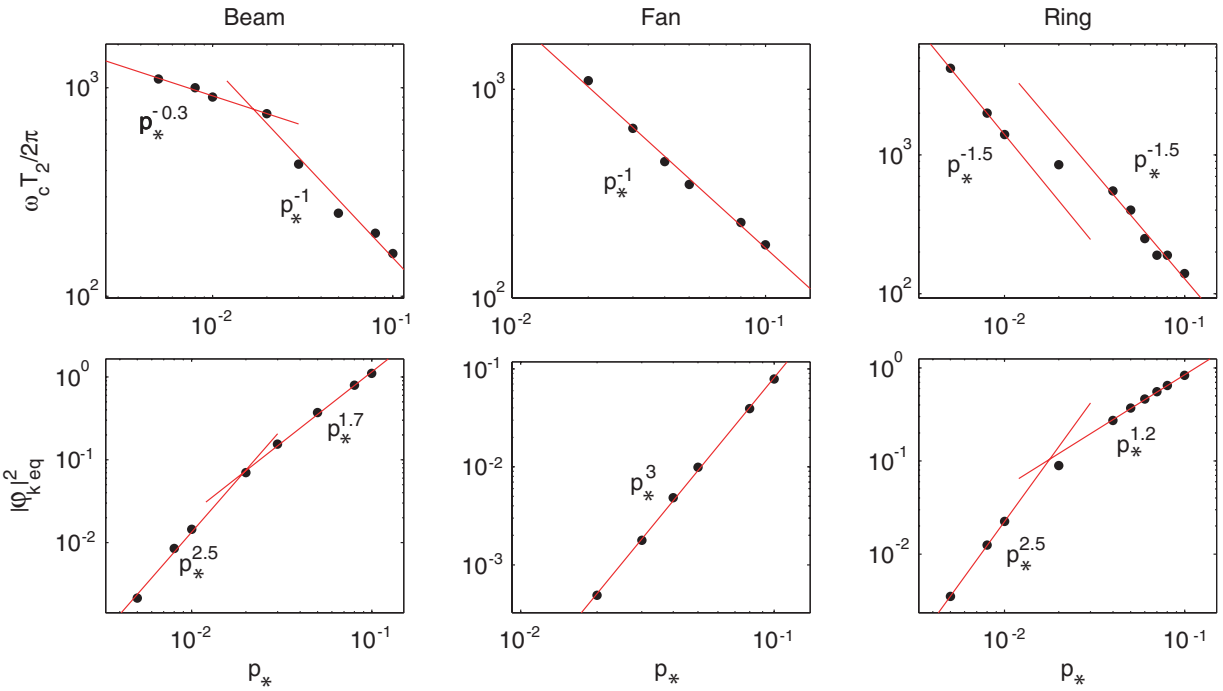

FIG. 14. (Color online) Interaction between two lower hybrid waves and a nonequilibrium electron distribution. Upper panels: variation of $\omega_c T_2/2\pi$ as a function of p_*, for different kinds of instabilities: beam, fan, and ring, as indicated in the figure. Lower panels: variation of the normalized mean value $|\varphi_{\mathbf{k}}|^2_{eq}$ around which the waves' amplitudes are oscillating at saturation, as a function of p_*, for the three types of instabilities. Corresponding p_*^β dependences are indicated as straight lines (all the axes have logarithmic scales). The main parameters are the same as in Fig. 4 (for the beam instability), Fig. 9 (for the ring instability), and Fig. 11 (for the fan instability).

$$T_{2r,k} \propto p_*^{0.2} \frac{N}{N_b(p_*)}. \tag{52}$$

In order to recover the scaling laws obtained for T_2 as a result of the numerical simulations (see Fig. 14), one has considered that the ratio $N_b(p_*)/N$ should lie within the range

$$p_*^{1.5} \lesssim \frac{N_b(p_*)}{N} \lesssim p_*^{0.7}, \quad p_* < 1, \tag{53}$$

an assumption which is reasonable, as for $p_*=0.1$ ($p_*=0.01$), $0.03 \lesssim N_b/N \lesssim 0.2$ ($0.001 \lesssim N_b/N \lesssim 0.04$).

As a conclusion, the simple model of two waves interacting resonantly with an electron bunch, which was presented in Sec. III, is shown to be in good qualitative agreement with the results provided by the 3D numerical simulations and to describe adequately the nontrivial dynamics of bunched resonant particles interacting simultaneously with two waves of close phase velocities. This result allows us to expect that the control of the processes of periodic exchanges of energy between waves via a common group of particles strongly interacting with them should lead to interesting applications, as the transformation of the energy carried by an electrostatic wave into electromagnetic radiation. Indeed, as explained in the Introduction, so-called "double resonance conditions" can be found for waves of different natures and are capable of different interaction mechanisms with resonant particles.

ACKNOWLEDGMENTS

The authors acknowledge the Centre National de la Recherche Scientifique (CNRS, France) and the Russian Academy of Sciences (Grant No. 06-02-72560-NCNIL_a) for their financial support.

APPENDIX A: INSTABILITY OF A WAVE WITH TRAPPED PARTICLES

Here we suppose that the particles' motion can be described in the frame of 1D geometry and limit ourselves to the case of the Landau resonance, $\omega=k_z v_z$. The motion of an electron in the potential $\varphi=\mathrm{Re}[\varphi_1 e^{-i(\omega_1 t-k_1 z)}+\varphi_2 e^{-i(\omega_2 t-k_2 z)}]$ of two waves (ω_1,k_1) and (ω_2,k_2) is described by

$$\frac{dp_z}{dt} = m_e \frac{dv_z}{dt} = e\ \mathrm{Re}[ik_1\varphi_1 e^{-i(\omega_1-k_1 v_{z0})t+i\zeta_1} + ik_2\varphi_2 e^{-i(\omega_2-k_2 v_{z0})t+i\zeta_2}],$$

$$\frac{dz}{dt} = v_z, \tag{A1}$$

where $\zeta_\alpha=k_\alpha(z-v_{z0}t)$ is the phase of the particle relatively to the wave α in the coordinate system moving with the phase velocity $v_{z0}=\omega_1/k_1$. Defining the electron velocity perturbation, $k_1\delta v_z=k_1(v_z-v_{z0})=d\zeta_1/dt$, and expressing ζ_2 with the help of $\zeta\equiv\zeta_1$, we get

$$\frac{d^2\zeta}{dt^2} = \frac{ek_1^2}{m_e}\mathrm{Re}\left(i\varphi_1 e^{i\zeta} + i\frac{k_2}{k_1}\varphi_2 e^{i\delta\omega t+i\zeta k_2/k_1}\right), \tag{A2}$$

where $\delta\omega=k_2 v_{z0}-\omega_2$. It is suitable to add the index p to ζ in order to distinguish each particle one from the other, and to introduce the notations

$$\varphi_\alpha = |\varphi_\alpha| e^{i\theta_\alpha},$$

$$\omega_{tr\alpha}^2 = \frac{ek_\alpha^2|\varphi_\alpha|}{m_e}. \tag{A3}$$

So, defining $\delta\omega_\alpha=k_\alpha v_{z0}-\omega_\alpha$, and with the help of Eq. (3) (see text), we get

$$\frac{d^2\zeta_p}{dt^2} = \omega_{tr1}^2\ \mathrm{Re}[ie^{i(\theta_1+\zeta_p)}] + \omega_{tr2}^2\ \mathrm{Re}\left[i\frac{k_1}{k_2}e^{i(\theta_2+\delta\omega t+\zeta_p k_2/k_1)}\right], \tag{A4}$$

$$\frac{d\varphi_\alpha}{dt} \simeq i\frac{8\pi e}{k_\alpha^2\,\partial\varepsilon_\alpha/\partial\omega_\alpha}\frac{n_{res}}{N}\sum_p e^{-i(\delta\omega_\alpha t+\zeta_p k_\alpha/k_1)}, \tag{A5}$$

where ε_α is the dielectric constant of the wave α. Let us consider an instability of the wave (ω_1,k_1), supposing that it remains in a steady state with the trapped particles and that it can be considered as a nonlinear BGK wave [21]. Below, only some properties of such a solution will be examined and used in the instability analysis. So, neglecting the influence of the second wave $(\varphi_2,\omega_{tr2}\to 0)$, the following equations have to be satisfied:

$$\frac{d^2\zeta_p}{dt^2} \simeq \omega_{tr1}^2\ \mathrm{Re}[ie^{i(\theta_1+\zeta_p)}], \tag{A6}$$

$$\left(\frac{d}{dt}+i\frac{d\theta_1}{dt}\right)|\varphi_1| - i\frac{8\pi e}{k_1^2\,\partial\varepsilon_1/\partial\omega_1}\frac{n_{res}}{N}\sum_p e^{-i(\zeta_p+\theta_1)} \simeq 0. \tag{A7}$$

Further we suppose that the bunches are well-formed, i.e., that the oscillations of the trapped particles are small, $|\zeta_p+\theta_1| \ll 1$, so that in the first approximation the solution of Eq. (A6) can be presented as oscillations at the bounce frequency ω_{tr1}

$$\zeta_p+\theta_1 \simeq a_p\cos(\omega_{tr1}t+\vartheta_p), \quad a_p \ll 1, \tag{A8}$$

where the amplitudes a_p and the phases ϑ_p $(p=1,N)$ are distributed to satisfy Eq. (A7), that is

$$|\varphi_1|\frac{d\theta_1}{dt} \simeq \frac{8\pi e n_{res}}{k_1^2\,\partial\varepsilon_1/\partial\omega_1},$$

$$\frac{d}{dt}|\varphi_1| \simeq \frac{8\pi e n_{res}}{k_1^2\,\partial\varepsilon_1/\partial\omega_1}\frac{1}{N}\sum_p(\zeta_p+\theta_1). \tag{A9}$$

Thus, for a steady state, the main wave (ω_1,k_1) acquires a nonlinear frequency shift

$$\frac{d\theta_1}{dt} = \delta\omega_{nl} \simeq \frac{8\pi e n_{res}}{|\varphi_1| k_1^2 \, \partial\varepsilon_1/\partial\omega_1}, \tag{A10}$$

which is due to the trapped particles. Note that there is no unique correspondence between the frequency shift $\delta\omega_{nl}$ and the wave amplitude $|\varphi_1|$. This fact is related to the features of the BGK mode solutions [21]. Then, according to well-known results on the asymptotic stage of the Landau damping of a finite amplitude wave [14], one can assume that the initial phases ϑ_p of the particles are distributed randomly so that

$$\frac{1}{N}\sum_p (\zeta_p + \theta_1) \simeq \langle a_p \cos(\omega_{tr1} t + \vartheta_p)\rangle = 0, \tag{A11}$$

showing that $\frac{d}{dt}|\varphi_1| \simeq 0$ [Eq. (A9)] is satisfied. The exact value of $\delta\omega_{nl}$ in the existing steady state is not essential for the instability analysis, and below we exclude it from our considerations by choosing a reference frame moving with the wave phase velocity corrected by the nonlinear frequency shift. In this coordinate frame, $\theta_1' = \theta_1 - \delta\omega_{nl} t$ is constant and so we can put $\theta_1' = 0$.

In the presence of a second wave of small amplitude ($\omega_{tr2} \ll \omega_{tr1}$, $\varphi_2 \neq 0$), the oscillations of the trapped particles are slightly perturbed

$$\zeta_p \simeq a_p \cos(\omega_{tr1} t + \vartheta_p) + \delta\zeta_p, \tag{A12}$$

where the small perturbation $\delta\zeta_p$ satisfies

$$\frac{d^2\delta\zeta_p}{dt^2} + \omega_{tr1}^2 \delta\zeta_p \simeq \omega_{tr1}^2 \frac{k_2}{k_1} \mathrm{Re}\left(i \frac{\varphi_2}{|\varphi_1|} e^{i(\delta\omega t + \zeta_p k_2/k_1)} \right). \tag{A13}$$

Then, keeping only terms which are linear on $\delta\zeta_p$, we get from Eq. (A5) ($\delta\omega = \delta\omega_2$)

$$\frac{d\varphi_2}{dt} \simeq i \frac{8\pi e}{k_2^2 \, \partial\varepsilon_2/\partial\omega_2} \frac{n_{res}}{N} e^{-i\delta\omega t} \sum_p \left(1 - i \frac{k_2}{k_1} a_p \cos(\omega_{tr1} t + \vartheta_p) \right) + \frac{8\pi e}{k_2^2 \, \partial\varepsilon_2/\partial\omega_2} \frac{k_2}{k_1} \frac{n_{res}}{N} e^{-i\delta\omega t} \sum_p \delta\zeta_p e^{-i(k_2/k_1) a_p \cos(\omega_{tr1} t + \vartheta_p)}. \tag{A14}$$

The first term in the right-hand side of Eq. (A14) does not depend on the perturbations of the particles' trajectories

$$i \frac{8\pi e}{k_2^2 \, \partial\varepsilon_2/\partial\omega_2} \frac{n_{res}}{N} e^{-i\delta\omega t} \sum_p \left(1 - i \frac{k_2}{k_1} a_p \cos(\omega_{tr1} t + \vartheta_p) \right) \simeq i \frac{8\pi e n_{res}}{k_2^2 \, \partial\varepsilon_2/\partial\omega_2} e^{-i\delta\omega t} \tag{A15}$$

and represents a forced response of the second wave to the modulated flux of trapped particles. It corresponds to the known fact that a nonlinear BGK wave is not a pure harmonic wave; the amplitudes of the harmonics $k' = mk_1$, $m = 2, \ldots$ are found from Eq. (A5),

$$\varphi_{k'} = -\frac{8\pi e}{\delta\omega_m k'^2 \, \partial\varepsilon/\partial\omega_{k'}} \frac{n_{res}}{N} \sum_p e^{-i[\delta\omega_m t + (k'/k_1)\zeta_p]}, \tag{A16}$$

and are supposed to be small, $|\varphi_{k'}| \ll |\varphi_1|$, if $|\delta\omega_m| = |\omega_1 - \omega_{k'} - v_{z0}(k_1 - k')| \gg |\delta\omega_{nl}|$. Here it is necessary to note that if the ratio k_2/k_1 of the second wave vector to the main wave vector is not an integer, such term vanishes, as it can be easily shown by calculating the corresponding Fourier harmonic of the trapped particle density $\delta n_e(z,t) = \Sigma_{n,p} \delta(z - n\lambda - vt - z_p)$,

$$\begin{aligned} \delta n_k &= \int \delta n_e(z,t) e^{-ikz} dz \\ &= \sum_{n,p} \int \delta(z - n\lambda - vt - z_p) e^{-ikz} dz \\ &= e^{-ikvt} \sum_n e^{-ikn\lambda} \sum_p e^{-ikz_p}, \end{aligned} \tag{A17}$$

where $\lambda = 2\pi/k_1$. As in the unperturbed state the coordinate z_p does not depend on the bunch number n, one can see that $\delta n_k \propto \Sigma_n e^{-ikn\lambda} = \Sigma_n e^{-2\pi i n(k/k_1)} = 0$ if k/k_1 is not an integer. If the trapped particles' oscillations are perturbed by the second wave, the perturbation δz_p depends on the bunch number and $\delta n_k \propto e^{-ikvt} \Sigma_n e^{-ikn\lambda} \Sigma_p \delta z_{pn}$ does not vanish. This corresponds to the last term in Eq. (A14).

One should also note that in the 1D case, if two waves have identical wave vectors, they have also the same or slightly different frequencies and it is not possible to consider them as two different waves: there is only one single wave; but, for a 3D geometry and in the presence of a background magnetic field, two waves can have the same k_z but different frequencies. This is exactly what we consider here in this simplified 1D description; so we can assume that the two waves are different even if $k_1 = k_2$. In this case it is not possible to omit the first term in the right-hand side of Eq. (A14), but if the frequency mismatch is large enough, it can be excluded from the instability analysis because in the linear approach it produces a partial nongrowing solution of Eq. (A14). Only the case $\delta\omega \simeq 0$ requires a special consideration, but it corresponds to the condition of double resonance that is examined in this paper on the basis of a nonlinear description of the wave-particle interaction.

Let us consider the situation when all particles oscillate near the bottom of the potential of the main wave, supposing that, in a first approach, it is possible to neglect the amplitude of the unperturbed displacement of the trapped particles. Thus we get from Eqs. (A13) and (A14) that

$$\frac{d^2\delta\zeta_p}{dt^2} + \omega_{tr1}^2 \delta\zeta_p \simeq \frac{k_2}{k_1} \omega_{tr1}^2 \, \mathrm{Re}\left(i \frac{\varphi_2}{|\varphi_1|} e^{i\delta\omega t} \right), \tag{A18}$$

$$\frac{d\varphi_2}{dt} \simeq \frac{8\pi e}{k_2^2 \, \partial\varepsilon_2/\partial\omega_2} \frac{k_2}{k_1} \frac{n_{res}}{N} e^{-i\delta\omega t} \sum_p \delta\zeta_p. \tag{A19}$$

Moreover, in the above assumption all particles are moving synchronously, and so $\frac{1}{N}\Sigma_p \delta\zeta_p \simeq \delta\zeta_p$. Then, introducing the solution of Eq. (A19),

$$\varphi_2 e^{i\delta\omega t} \simeq \int^t \frac{8\pi e n_{res}}{k_2^2\, \partial\varepsilon_2/\partial\omega_2} \frac{k_2}{k_1} e^{i\delta\omega(t-t')} \delta\zeta_p(t')dt', \quad \text{(A20)}$$

in Eq. (A18), one gets

$$\frac{d^2\delta\zeta_p}{dt^2} + \omega_{tr1}^2 \delta\zeta_p \simeq \omega_{tr1}^2 \frac{k_2^2}{k_1^2} \frac{8\pi e n_{res}}{|\varphi_1| k_2^2\, \partial\varepsilon_2/\partial\omega_2} \times \mathrm{Re}\left(i \int^t e^{i\delta\omega(t-t')} \delta\zeta_p(t')dt' \right). \quad \text{(A21)}$$

Searching growing solutions of the form $\delta\zeta_p = Ae^{-i\Omega t} + \text{c.c.}$, one finds that

$$(\omega_{tr1}^2 - \Omega^2) Ae^{-i\Omega t} + \text{c.c.} \simeq -\omega_{tr1}^2 \frac{k_2^2}{k_1^2} \frac{8\pi e n_{res}}{|\varphi_1| k_2^2\, \partial\varepsilon_2/\partial\omega_2} \mathrm{Re}\left(\frac{Ae^{-i\Omega t}}{\delta\omega + \Omega} + \frac{A^* e^{i\Omega^* t}}{\delta\omega - \Omega^*} \right) \quad \text{(A22)}$$

$$\simeq -\frac{1}{2}\omega_{tr1}^2 \frac{k_2^2}{k_1^2} \frac{8\pi e n_{res}}{|\varphi_1| k_2^2\, \partial\varepsilon_2/\partial\omega_2} \left[\left(\frac{1}{\delta\omega + \Omega} + \frac{1}{\delta\omega - \Omega} \right) Ae^{-i\Omega t} + \text{c.c.} \right], \quad \text{(A23)}$$

where A^* (Ω^*) is the complex conjugate of A (Ω). Finally we get the dispersion relation which determines the growth rate of the second (sideband) wave and the perturbation of the particles' oscillations

$$\Omega^2 - \omega_{tr1}^2 \simeq \omega_{tr1}^2 \frac{k_2}{k_1} \frac{4\pi e n_{res}}{|\varphi_1| k_2^2\, \partial\varepsilon_2/\partial\omega_2} \left(\frac{1}{\delta\omega + \Omega} + \frac{1}{\delta\omega - \Omega} \right). \quad \text{(A24)}$$

Taking into account the difference of notations and definitions, one can see that Eq. (A24) has some similarity with the equation obtained for the sideband instability in Ref. [3]. Indeed, noting that (we use hereafter $\varepsilon \equiv \varepsilon_2$)

$$\frac{\partial\varepsilon}{\partial\omega_2}(\delta\omega + \Omega, k_2) = \frac{\partial\varepsilon}{\partial\omega_2}(\Omega + k_2 v_{z0} - \omega_2, k_2) \simeq \varepsilon(\Omega + k_2 v_{z0}, k_2), \quad \text{(A25)}$$

and owing to the property of the dielectric permittivity $\varepsilon^*(-\omega^*, -k) = \varepsilon(\omega, k)$ [25], one gets

$$\begin{aligned} \varepsilon(\Omega + k_2 v_{z0} - 2\omega_1, k_2 - 2k_1) &\simeq [\varepsilon(2\omega_1 - k_2 v_{z0} - \Omega^*, 2k_1 - k_2)]^* \\ &\simeq \frac{\partial\varepsilon}{\partial\omega_2}(2\omega_1 - k_2 v_{z0} - \Omega^* - \omega_2)^* \\ &\simeq \frac{\partial\varepsilon}{\partial\omega_2}[v_{z0}(2k_1 - k_2) - \Omega^* - \omega_2]^* \\ &\simeq \frac{\partial\varepsilon}{\partial\omega_2}(\delta\omega - \Omega), \end{aligned} \quad \text{(A26)}$$

where we took into account that $k_1 \simeq k_2$ and neglected the small imaginary part of the dielectric permittivity ε. Then, defining $\Omega + k_2 v_{z0} \to \omega$ and $\omega_{p,res}^2 = 4\pi e^2 n_{res}/m_e$, Eq. (A24) can be rewritten at $k_1/k_2 = 1$ in the form presented in Ref. [3].

$$1 \simeq \frac{\omega_{p,res}^2}{\Omega^2 - \omega_{tr1}^2} \left(\frac{1}{\varepsilon(\omega, k_2)} + \frac{1}{\varepsilon(\omega - 2\omega_1, k_2 - 2k_1)} \right). \quad \text{(A27)}$$

However, one has to stress that the result (A27) of Kruer *et al.* [3] and Eq. (A24) are not identical. This can be explained by the fact that two different problems are investigated. Kruer *et al.* suppose that at initial time, except of the main wave trapping particles, there are many other waves with different wave vectors and quite small amplitudes. Among this set of waves, there are only two waves which are unstable and grow. On the contrary, the present paper supposes that except the main wave, there is only one other wave and its aim is to find the conditions when this wave is unstable.

The growth rate $\gamma = \mathrm{Im}(\Omega)$ can be calculated supposing that $-\mathrm{Re}(\Omega) \simeq \omega_{tr1} \gg \gamma$. Assuming that only one satellite wave (so-called red wave) is growing and neglecting correspondingly the second term in the right-hand side of Eq. (A24), one can see from

$$(\omega_{tr1}^2 - \Omega^2)(\delta\omega + \Omega) \simeq 2i\gamma\omega_{tr1}(\delta\omega + \Omega) = -\frac{k_1}{k_2} \frac{4\pi e^2 n_{res}}{m_e\, \partial\varepsilon/\partial\omega_2} \quad \text{(A28)}$$

that the maximum growth rate $\gamma_{\max}$ is reached at $\delta\omega \simeq \omega_{tr1}$ and is expressed as

$$\gamma_{\max} \simeq \sqrt{\frac{k_1}{2k_2} \frac{4\pi e^2 n_{res}}{\omega_{tr1} m_e\, \partial\varepsilon/\partial\omega_2}} \simeq \sqrt{\frac{\omega_{p,res}^2}{2\omega_{tr1}\, \partial\varepsilon/\partial\omega_2}}. \quad \text{(A29)}$$

Note that the same growth rate can be obtained for the blue satellite wave if one keeps the second term on the right-hand side in Eq. (A24). Using the obtained solution, one can see that the second term omitted in Eq. (A24) is small if $\omega_{p,res}^2 \ll \omega_{tr1}^3 \frac{\partial\varepsilon}{\partial\omega_2}$; in the opposite case, both the red and blue satellite waves overlap, which means that their growth rates become of the same order as the difference between their frequencies.

APPENDIX B: HAMILTONIAN DESCRIPTION OF THE BUNCH-WAVES SYSTEM

1. Hamiltonian formalism for wave-particle interaction

When the nonlinear coupling between the waves can be neglected compared to their interactions with the particles, the Hamiltonian $\mathcal{H}$ describing a group of N resonant electrons interacting with a packet of N_w electrostatic waves $(\omega_{\mathbf{k}}, \mathbf{k})$ in a magnetized plasma is given by [19]

$$\mathcal{H} = \sum_{p=1}^{N} \mathcal{H}_p + \sum_{\mathbf{k}}^{N_w} \mathcal{H}_{\mathbf{k}} - \sum_{p=1}^{N} \sum_{\mathbf{k}}^{N_w} e\Phi_{\mathbf{k}p}. \quad \text{(B1)}$$

Let us detail each term of this Hamiltonian, keeping in mind the notations of Sec. II: $\mathbf{r}_p = (x_p, y_p, z_p)$ is the position of the

particle p, $\mathbf{v}_p=(v_{xp},v_{yp},v_{zp})$ is its velocity, and $\varphi_{\mathbf{k}}$ is the slow varying complex amplitude of the potential of the wave $(\omega_{\mathbf{k}},\mathbf{k})$. $\mathcal{H}_p$ is the kinetic energy of the nonrelativistic electron p moving in the ambient magnetic field $\mathbf{B}_0=B_0\mathbf{z}$, that can be written using the angle-action formalism as

$$\mathcal{H}_p=\frac{p_{zp}^2}{2m_e}+\omega_c J_p, \tag{B2}$$

where $p_{zp}=m_e v_{zp}$ is the parallel momentum of the particle and $J_p=m_e(v_{xp}^2+v_{yp}^2)/2\omega_c$ is its magnetic momentum. $\mathcal{H}_{\mathbf{k}}$ is the energy of the plasma eigenmode $(\omega_{\mathbf{k}},\mathbf{k})$, that is

$$\mathcal{H}_{\mathbf{k}}=\omega_{\mathbf{k}}I_{\mathbf{k}}, \tag{B3}$$

where $I_{\mathbf{k}}=|\varphi_{\mathbf{k}}|^2/2\eta_{\mathbf{k}}$ is the canonical action of the wave and $\eta_{\mathbf{k}}$ depends on the wave dispersion as

$$\eta_{\mathbf{k}}=\frac{8\pi}{V\mathbf{k}^2}\left(\frac{\partial\varepsilon(\mathbf{k},\omega_{\mathbf{k}})}{\partial\omega_{\mathbf{k}}}\right)^{-1}. \tag{B4}$$

The last term in Eq. (B1) describes the interaction between the particles and the waves and can be written as

$$\Phi_{\mathbf{k}p}=(2\eta_{\mathbf{k}}I_{\mathbf{k}})^{1/2}\cos(\mathbf{k}\cdot\mathbf{r}_p-\phi_{\mathbf{k}}), \tag{B5}$$

with $\mathbf{k}\cdot\mathbf{r}_p=\mathbf{k}\cdot\mathbf{R}_p+(2J_p/m_e\omega_c)^{1/2}(k_x\cos\theta_p+k_y\sin\theta_p)$ and $\mathbf{R}_p=(X_p,Y_p/m_e\omega_c,z_p)$; (Y_p,X_p), (J_p,θ_p), and (p_{zp},z_p) are the conjugated pairs of momenta and positions; $\mathbf{R}_p$ is the guiding center position of the particle p, and $\theta_p=-\arctan(v_{xp}/v_{yp})$ is the azimuthal angle associated to the action J_p. The wave phase $\phi_{\mathbf{k}}=\omega_{\mathbf{k}}t-\arg(\varphi_{\mathbf{k}})$ is canonically conjugated to $I_{\mathbf{k}}$.

In order to make the cyclotron resonances appear explicitely, we expand the interaction term in Fourier series with respect to the angle θ_p, using $e^{ix\sin\theta}=\Sigma_{n=-\infty}^{+\infty}J_n(x)e^{in\theta}$, where $J_n(x)$ is the Bessel function of integer order n. Introducing the angle $\theta_{\mathbf{k}}$ so that $k_x=k_\perp\sin\theta_{\mathbf{k}}$ and $k_y=k_\perp\cos\theta_{\mathbf{k}}$, as well as the Larmor radius $\rho_p=(2J_p/m_e\omega_c)^{1/2}$ of the particle p, one obtains

$$\Phi_{\mathbf{k}p}=(2\eta_{\mathbf{k}}I_{\mathbf{k}})^{1/2}\sum_{n=-\infty}^{+\infty}J_n(k_\perp\rho_p)\cos[\mathbf{k}\cdot\mathbf{R}_p+n(\theta_p+\theta_{\mathbf{k}})-\phi_{\mathbf{k}}], \tag{B6}$$

showing that the cyclotron resonance condition for the particle p and the wave $(\omega_{\mathbf{k}},\mathbf{k})$ is $k_z z_p+n\theta_p-\phi_{\mathbf{k}}\simeq$ const, i.e., $k_{z\alpha}v_z\simeq\omega_{\mathbf{k}}-n\omega_c$.

The evolution of the system is then obtained by using the Hamilton equations $dp/dt=-\partial\mathcal{H}/\partial q$ and $dq/dt=\partial\mathcal{H}/\partial p$, where (p,q) are the pairs of canonically conjugated variables. One can check that the parallel momentum $\mathcal{P}$ of the system is a constant of the motion

$$\mathcal{P}=\sum_{\mathbf{k}}k_z I_{\mathbf{k}}+\sum_p p_{zp}=\text{const}. \tag{B7}$$

2. Bunch-waves system

Let us consider the case of one bunch (that is, a single macroparticle) formed by N_b resonant particles moving synchronously in the potential of N_w electrostatic waves defined by the angle-action variables (I_α,ϕ_α), the frequencies and wave vectors $(\omega_\alpha,\mathbf{k}_\alpha)$, as well as the interaction parameters η_α [Eq. (B4)], where $\alpha=1,\ldots,N_w$. The Hamiltonian (B1) of this bunch-waves system can be decomposed as follows:

$$\mathcal{H}=\left(\sum_{p=1}^{N_b}\mathcal{H}_p+\sum_{p=N_b+1}^{N}\mathcal{H}_p\right)+\sum_{\mathbf{k}}\mathcal{H}_{\mathbf{k}}-e\sum_{\mathbf{k}}\left(\sum_{p=1}^{N_b}\Phi_{\mathbf{k}p}+\sum_{p=N_b+1}^{N}\Phi_{\mathbf{k}p}\right), \tag{B8}$$

where one can assume that $e\Sigma_{\mathbf{k}}\Sigma_{p=N_b+1}^{N}\Phi_{\mathbf{k}p}\simeq 0$ and $\Sigma_{p=N_b+1}^{N}\mathcal{H}_p\simeq$ const as the $N-N_b$ resonant electrons which do not belong to the bunch are submitted to phase mixing. Note that we ignore here the influence of the trapped phase-mixed particles on the waves' evolution and therefore on the motion of the trapped bunched particles. Thus the system can be described by the Hamiltonian $\mathcal{H}_b$,

$$\mathcal{H}_b=\sum_{p=1}^{N_b}\left(\frac{p_{zp}^2}{2m_e}+\omega_c J_p\right)+\sum_{\alpha}(\omega_\alpha I_\alpha-e\sum_{p=1}^{N_b}\mathrm{Re}[(2\eta_\alpha I_\alpha)^{1/2}e^{i(\mathbf{k}_\alpha\cdot\mathbf{r}_p-\phi_\alpha)}]), \tag{B9}$$

where the momenta and the positions of all the bunched particles are equal, i.e., $p_{zp}=p_z$, $J_p=J$, and $\mathbf{r}_p=\mathbf{r}$ for $p=1,\ldots,N_b$. Then one can define new canonical variables (P_b,Z_b), (J_b,θ_b), and (Y_b,X_b) representing the bunch's conjugate momenta and positions,

$$\begin{aligned}P_b&=N_b p_z,\\ J_b&=N_b J,\\ Y_b&=N_b Y,\\ Z_b&=\frac{1}{N_b}\sum_{p=1}^{N_b}z_p=z,\\ \theta_b&=\theta,\\ X_b&=X.\end{aligned} \tag{B10, B11}$$

Avoiding the $3(N_b-1)$ degrees of freedom owing to the $3(N_b-1)$ independent constraints $p_p=P_b$ and $\mathbf{r}_p=\mathbf{r}_b$, one obtains

$$\mathcal{H}_b=\frac{P_b^2}{2N_b m_e}+\omega_c J_b+\sum_\alpha\{\omega_\alpha I_\alpha-eN_b\,\mathrm{Re}[(2\eta_\alpha I_\alpha)^{1/2}e^{i(\mathbf{k}_\alpha\cdot\mathbf{r}_b-\phi_\alpha)}]\}. \tag{B12}$$

Note that $\mathcal{H}_b$ [Eq. (B12)] is similar to the Hamiltonian describing the interaction between the waves and a single particle of mass $M_b=N_b m_e$ and charge $-q_b=-N_b e$. Below we will use such notations and only express the final results in terms of m_e, e, and N_b.

In order to simplify the problem, let us consider that all the bunched particles are moving with a velocity close to the resonance velocity defined by $k_{z\alpha}P_b(t=0)/m_e+n\omega_c-\omega_\alpha\simeq 0$, for all the waves α (what is justified by the trapping mechanism), and let us neglect the influence of the other resonances by keeping only the contribution of the resonance n, $\exp[i(\mathbf{k}_\alpha\cdot\mathbf{r}_b-\phi_\alpha)]\simeq J_n(k_{\perp\alpha}\rho_b)\exp\{i[\mathbf{k}_\alpha\cdot\mathbf{R}_b+n(\theta_b+\theta_\alpha)-\phi_\alpha]\}$. Note that in the most realistic case where only two waves are considered ($\alpha=1$, $\alpha'=2$), it follows from $d\mathbf{k}_\alpha\cdot\mathbf{R}_\perp/dt=(e/m_e\omega_c)(2\eta_{\alpha'}I_{\alpha'})^{1/2}\sin(\mathbf{k}_{\alpha'}\cdot\mathbf{r}_p-\phi_{\alpha'})[k_{x\alpha}k_{y\alpha'}-k_{y\alpha}k_{x\alpha'}]$ that $\mathbf{k}_\alpha\cdot\mathbf{R}_\perp=\text{const}$ ($\alpha=1,2$) if $\mathbf{k}_{\perp 1}\times\mathbf{k}_{\perp 2}=0$; then the degree of freedom associated with the perpendicular particles' drift can be avoided. The angles θ_α verifying $k_{x\alpha}=k_{\perp\alpha}\sin\theta_\alpha$ and $k_{y\alpha}=k_{\perp\alpha}\cos\theta_\alpha$ can also be included as an initial condition in the waves' phases by defining $I'_\alpha=I_\alpha$ and $\phi'_\alpha=\phi_\alpha-\mathbf{k}_\alpha\cdot\mathbf{R}_\perp-n\theta_\alpha$. Then the Hamiltonian is

$$\mathcal{H}_b=\frac{P_b^2}{2M_b}+\omega_c J_b+\sum\nolimits_\alpha\omega_\alpha I'_\alpha - q_b\,\mathrm{Re}\sum\nolimits_\alpha(2\eta_\alpha I'_\alpha)^{1/2}J_n(k_{\perp\alpha}\rho_b)e^{i(k_{z\alpha}Z_b+n\theta_b-\phi'_\alpha)}, \tag{B13}$$

and after performing several canonical transformations, we get (omitting primes)

$$\mathcal{H}_{b,n}=\frac{\left(\mathcal{P}-\sum_\alpha k_{z\alpha}I_\alpha\right)^2}{2M_b}+\omega_c\mathcal{J}+\sum\nolimits_\alpha(\omega_\alpha-n\omega_c)I_\alpha - q_b\sum\nolimits_\alpha(2\eta_\alpha I_\alpha)^{1/2}J_n(k_{\perp\alpha}\rho_b)\cos\phi_\alpha, \tag{B14}$$

where $I_\alpha=|\varphi_\alpha|^2/2\eta_\alpha$ and $\phi_\alpha=\omega_\alpha t-\arg(\varphi_\alpha)-k_{z\alpha}Z_b-\mathbf{k}_{\perp\alpha}\cdot\mathbf{R}_{\perp b}-n(\theta_b+\theta_\alpha)$. The bunch's Larmor radius ρ_b is

$$\rho_b(I_\alpha)=(2J_b/M_b\omega_c)^{1/2}=\left[\frac{2}{M_b\omega_c}\left(\mathcal{J}-n\sum\nolimits_\alpha I_\alpha\right)\right]^{1/2}. \tag{B15}$$

The generalized momenta $\mathcal{J}=J_b+n\Sigma_\alpha I_\alpha$ and $\mathcal{P}=P_b+\Sigma_\alpha k_{z\alpha}I_\alpha$ are constants of the motion (their conjugated variables Z_b and θ_b do not appear explicitly in $\mathcal{H}_{b,n}$). Note that in Eq. (B14) the parallel kinetic energy of the bunch plays the role of a wave-wave interaction energy and that the coherent motion of the bunched particles can generate some coupling between the waves. The bunch Larmor radius ρ_b may also play this role in the case of the cyclotron resonances $n\neq 0$ [Eqs. (B14) and (B15)].

Let us now focus our attention to the case when only two waves are present, in order to point out a specific coupling mechanism responsible for the periodic exchanges of energy between the waves. The Hamiltonian equations provide, using Eq. (B14) and taking into account Eq. (B15), that

$$\frac{d}{dt}I_\alpha=-\frac{\partial}{\partial\phi_\alpha}\mathcal{H}_{b,n}=-q_b(2\eta_\alpha I_\alpha)^{1/2}J_n(k_{\perp\alpha}\rho_b)\sin\phi_\alpha, \tag{B16}$$

$$\frac{d}{dt}\phi_\alpha=\frac{\partial}{\partial I_\alpha}\mathcal{H}_{b,n} =(\omega_\alpha-n\omega_c)-\frac{k_{z\alpha}}{M_b}(\mathcal{P}-k_{z1}I_1-k_{z2}I_2) - q_b\cos\phi_\alpha\left[(\eta_\alpha/2I_\alpha)^{1/2}J_n(k_{\perp\alpha}\rho_b) - (2\eta_\alpha I_\alpha)^{1/2}\frac{dJ_n(k_{\perp\alpha}\rho_b)}{dI_\alpha}\right], \tag{B17}$$

where $\alpha=1,2$. For the Landau resonance $n=0$, the last term in Eq. (B17) vanishes, as $\rho_b=(2\mathcal{J}/M_b\omega_c)^{1/2}=\text{const}$. Then the only coupling between the waves results from the parallel motion of the bunch. Supposing that $k_{\perp\alpha}\rho_b<1$, i.e., $J_0(k_{\perp\alpha}\rho_b)\simeq 1$, the system can be described by the Hamiltonian

$$\mathcal{H}_{b,0}=\frac{\left(\mathcal{P}-\sum_\alpha k_{z\alpha}I_\alpha\right)^2}{2M_b}+\omega_c\mathcal{J} + \sum\nolimits_\alpha[\omega_\alpha I_\alpha-q_b(2\eta_\alpha I_\alpha)^{1/2}\cos\phi_\alpha]. \tag{B18}$$

The case of cyclotron resonances $n\neq 0$ is more complicated, as the last term in Eq. (B17) contributes to the coupling (modification of the frequency detuning due to the particles)

$$\frac{d}{dI_\alpha}J_n(k_{\perp\alpha}\rho_b)=k_{\perp\alpha}J'_n(k_{\perp\alpha}\rho_b)\frac{d\rho_b}{dI_\alpha}=-\frac{nk_{\perp\alpha}}{M_b\omega_c\rho_b}J'_n(k_{\perp\alpha}\rho_b). \tag{B19}$$

Let us show that, for the resonances $n=\pm 1$, this coupling is in most cases negligible. For the ring instability at the normal cyclotron resonance ($n=1$), the particles which interact strongly with the waves verify $J'_1(k_{\perp}\rho_b)\simeq 0$, that is, $k_{\perp\alpha}\rho_b\simeq 1.8$ [23]; then it is not necessary to take into account the last term in Eq. (B17) and one can suppose that $J_1(k_{\perp\alpha}\rho_b)\simeq\text{const}$. The validity of this assumption has been checked with the help of numerical simulations. For the fan instability at the anomalous cyclotron resonance ($n=-1$), assuming that $k_{\perp\alpha}$ is large enough so that $k_{\perp\alpha}\rho_b<1$ for all particles in the bunch, one can write $J_{-1}(k_{\perp\alpha}\rho_b)\simeq -k_{\perp\alpha}\rho_b/2$ which provides for Eq. (B17) that

$$\frac{d}{dt}\phi_\alpha=(\omega_\alpha+\omega_c)-\frac{k_{z\alpha}}{M_b}(\mathcal{P}-k_{z1}I_1-k_{z2}I_2) + k_{\perp\alpha}q_b\left[(\eta_\alpha/8I_\alpha)^{1/2}\rho_b+\frac{1}{M_b\omega_c}\frac{(\eta_\alpha I_\alpha/2)^{1/2}}{\rho_b}\right]\cos\phi_\alpha. \tag{B20}$$

[1] V. D. Shapiro and V. I. Shevchenko, Sov. Phys. JETP **30**, 1121 (1970).
[2] A. A. Galeev and R. Z. Sagdeev, *Reviews of Plasma Physics* (Consultants Bureau, New York, 1975).
[3] W. L. Kruer, J. M. Dawson, and R. N. Sudan, Phys. Rev. Lett. **23**, 838 (1969).
[4] W. L. Kruer and J. M. Dawson, Phys. Fluids **13**, 2747 (1970).
[5] M. V. Goldman, Phys. Fluids **13**, 1281 (1970).
[6] J. Denavit, Phys. Fluids **28**, 2773 (1985).
[7] A. B. Kitsenko, I. M. Pankratov, and K. N. Stepanov, Plasma Phys. **17**, 173 (1975).
[8] G. Dimonte and J. H. Malmberg, Phys. Fluids **21**, 1188 (1978).
[9] D. A. Hartmann and C. F. Driscoll, Phys. Plasmas **8**, 3457 (2001).
[10] V. N. Tsytovich, *Nonlinear Effects in Plasmas* (Plenum, New York, 1970).
[11] A. Volokitin and C. Krafft, Phys. Plasmas **11**, 3165 (2004).
[12] C. Krafft, A. Volokitin, and A. Zaslavsky, Phys. Plasmas **12**, 112309 (2005).
[13] W. E. Drummond, J. H. Malmberg, T. M. O'Neal, and J. R. Thompson, Phys. Fluids **13**, 2422 (1970).
[14] T. M. O'Neil, J. H. Winfrey, and J. H. Malmberg, Phys. Fluids **14**, 1204 (1971).
[15] N. G. Matsiborko, I. N. Onishchenko, V. D. Shapiro, and V. I. Shevchenko, Plasma Phys. **14**, 591 (1972).
[16] H. E. Mynick and A. N. Kaufman, Phys. Fluids **21**, 653 (1978).
[17] A. Zaslavsky, C. Krafft, and A. Volokitin, Phys. Rev. E **73**, 016406 (2006).
[18] M-C. Firpo, F. Doveil, Y. Elskens, P. Bertrand, M. Poleni, and D. Guyomarc'h, Phys. Rev. E **64**, 026407 (2001).
[19] Y. Elskens and D. Escande, *Microscopic Dynamics of Plasmas and Chaos* (Institute of Physics, University of Reading, Berkshire, 2003).
[20] E. G. Evstatiev, W. Horton, and P. J. Morrison, Phys. Plasmas **10**, 4090 (2003).
[21] I. B. Bernstein, J. M. Greene, and M. D. Kruskal, Phys. Rev. **108**, 546 (1957).
[22] T. Stix, *Waves in Plasmas* (Springer-Verlag, New York, 1992).
[23] A. Volokitin and C. Krafft, Ann. Geophys. **21**, 1393 (2003).
[24] A. Zaslavsky, C. Krafft, and A. Volokitin, Phys. Plasmas **14**, 122302 (2007).
[25] L. D. Landau, E. M. Lifshitz, and L. P. Pitaevskii, *Electrodynamics of Continuous Media*, 2nd ed. (Butterworth-Heinemann, London, 1984).